Acetylene-filled pressure broadened short photonic microcells

by

Sajed Hosseini-Zavareh

B.S., Kharazmi university of Tehran, 2014

A THESIS

submitted in partial fulfillment of the requirements for the degree

MASTER OF SCIENCE

Department of Physics
College of Arts and Sciences

KANSAS STATE UNIVERSITY
Manhattan, Kansas

2019

Approved by:

Major Professor
Kristan L. Corwin

Copyright

Abstract

We have developed short acetylene-filled photonic microcells (PMCs') as optical frequency references in the near infrared region for applications in telecommunication, gas sensing, and metrology. The PMC is a 5-10 cm long hollow-core photonic crystal fiber (HC-PCF) in which the high pressure acetylene gas is confined by sealing the ends of HC-PCF. Acetylene provides 50 strong $v_1 + v_3$ rotational-vibrational combination bands within 1510-1540 nm which covers the telecommunication window at 1550 nm.

PMC's are a possible replacement for optical frequency references based on gas-filled vapor cells, like the SRM2517a produced by the National Institute of Standards and Technology (NIST). While such cells made practical and accurate frequency calibration readily available, and have been built into measurement equipment and lasers, they are relatively bulky compared to the small footprint now achieved by commercially available lasers. Short PMC's in particular are compact and robust. In fact, a PMC of similar length would occupy a smaller volume because it has a simple design and it is all-fiber based.

Here we demonstrate a novel fabrication technique that is appropriate for making short high pressure optical frequency references using photonic bandgap fibers. Consequently, the aforementioned short PMC has some application of NIST SRM 2517a and can be used for moderate accuracy frequency measurements with fractional accuracy of 7.7×10^{-8}. By using a tapering technique to seal the microcells, we were able to achieve high transmission efficiency of 80% and moderate accuracy of 10 MHz (1σ) in finding the line center. This approaches that of the NIST SRM 2517a 10 MHz (2σ) accuracy. Using an earlier Q-tipping technique, 37% off-resonant transmission and 5 MHz accuracy were achieved in finding the line center, but a larger etalon-like effect which is approximately 13%, appears on the wings of the optical depth. By

using a tapering technique, we were able to decrease the etalon-like effect to less than 1%. In both cases, the microcells could be connectorized, albeit with reduction in off-resonant transmission efficiency, for integration into multi-mode fibers or free-space optical systems. Although contamination is introduced during both fabrication techniques, the P13 PMC line center shift with respect to sub-Doppler center is small according to experimental data. Data show that the PMC line center shift from the sub-Doppler feature for PMC no. 53 with 83% contamination was -15.4 ± 3.3 MHz which is a fractional value of 7.7×10^{-8} with respect to the value of the P13 line center of 195 THz. Finally, repeatable measurements show that PMCs are stable in terms of total pressure over approximately one year.

Table of Contents

List of Figures

List of Tables

Acknowledgements

First, I want to thank my supervisor Dr. Kristan Corwin. She has been a great mentor, wise researcher, a good friend, and she has an excellent personality. This work was not done without Dr. Corwin's support.

Second, I want to thank Dr. Brian Washburn one of my committee members who was like a supervisor for me and helped me with my research. He is a great and very smart teacher. Not only I learned a lot from him in nonlinear optics course, but also I learned a lot about optics and research collaborating with him.

Anyways, you two are nice couples and I am going to miss you wherever you are. I hope to meet you one day again and I wish you success and happiness. I am so proud of you.

There is one little big man who is going to have a great future like his parents Dr. Corwin and Washburn and that is Logan. Yes, I heard what you said to Kristan and I will not forget you. I want to thank you as part of our group. You are going to have a great future. I am sure about it.

Next, I owe my special thanks to Dr. Cosmin Blaga as my next supervisor and my committee member for giving me creative and nice feedbacks. I am so excited to learn from him in research. He is a nice person as well.

I like to thank my colleagues Neda Dadashzedeh, Kushan Weerasinghe, Manasadevi Thirugnanasambandam, Ryan Luder, Lindsay Hutcherson, and Chenchen Wang. We had such a great time together that I will never forget.

There are too many friends and professors who had a lot of impact on me and I was impressed by their great personalities during this long journey. If I want to write their names here, it is going to take more than the pages of this thesis. Therefore, I want to thank all of my

friends and professors, especially people from Manhattan Kansas, Boulder Colorado and back in my country. Thanks for all your support and advice.

This work was supported by the Air Force Office of Scientific Research (AFOSR) through grant (FA9550-14-1-0024), and Sorensen Incubator funding. We thank Dr. Jason Ensher and his colleagues from Insight optics for their contribution to this work. We acknowledge staff of the James R. Macdonald laboratory for helpful technical contributions, specially Chris Aikens and Justin Millette.

I want to thank my best english teacher Mohsen Nazaran and his wife Mahboube Azad for hosting me and having one of the best moments with them in Wichita. What a small world we are living in. Sir Nazaran you are a great mentor for me.

Well, finally the most difficult part is thanking my family because I do not know how to express my feelings about how supportive you are and how blessed I am to have you. I want to specially thank my excellent mom (Shahla Jalili), dad (Mansour Hosseini-Zavareh), and my brother (Hamed Hosseini-Zavareh). I appreciate all your support and help. You are the first reason for all the credits I achieve. Part of my success I achieve is because of my family who lives in America and I spent most of my time with them. For that, I would like to thank my grandmother Batoul Zahmatkesh who I spent part of my life living with her back in my country and she was like a mother for me. It has been a great pleasure to have the opportunity to visit her here in the United States of America. Thanks to my Uncles, Vahid and Saeid Jalili. Especially, Vahid who have his support. Vahid has been like a father for me and he has been next to me during the most critical situations in my life. Additionally, I like to thank my great Samani family as part of my journey in America who I have spent precious moments with them. Dear Raha, Reza, Raya, Behzad, Helia, Sam, Azadeh, Kathy, Shahnaz, and Narges we have had

invaluable moments together and I hope to see you again. Dear Raha you have been always so nice to me and I do not know how to put this kindness into words. I never forget you and Reza wherever I am. Furthermore, I want to thank my aunt Rouhangiz Nasirzadeh and my cousins Ramin and Yassi.

Dedication

This Thesis is dedicated to my mother (Shala Jalili), my father (Mansour Hosseini-Zavareh), my brother (Hamed Hosseini-Zavareh), my grandmother (Batoul Zahmatkesh), my uncles (Vahid and Saeid Jalili), my aunt (Rouhangiz Nasirzadeh), and Raha Samani.

Preface

This thesis is based on the research done by my previous colleagues Kevin Knabe, Chenchen Wang, and Rajesh Thapa. Here I focused on the novel fabrication technique of making short photonic microcells and their characterization. For more detailed theoretical information the best reference would be the book written by Demtroder [1].

To have a general idea of research done by my colleagues one could check Rajesh Thapa's master report [2] (specifically, the theoretical background and molecular spectroscopy of acetylene chapters), Kevin Knabe's PhD thesis [3] (specially chapters 2,5, Appendix A,B, and C), and Chechen Wang's PhD thesis [4] (specially chapters 2,5,6 and Appendix D).

Furthermore, I found Dr. Washburn's PhD thesis [5] useful in my research for the theoretical and historical optics background.

Chapter 1 - Introduction

Acetylene gas has about 50 molecular ro-vibrational absorption lines between 1510 nm and 1540 nm which makes it a useful optical reference in the near Infrared (IR) telecommunication band [6]. The aforementioned telecommunication band which is called the C-band refers to the wavelength range of 1530 nm to 1565 nm and it correlated to the amplification range of erbium doped fiber amplifiers (EDFAs). Consequently, pressure broadened acetylene vapor cells such as NIST Standard Reference Material (SRM) 2517 described in Swann *et al.* [7] are used to calibrate tunable laser frequencies, optical spectrum analyzers, and other light sources in the near IR region. This fiber-coupled glass cell has a pressure of 50 torr which provides 15 lines with uncertainties of approximately 10 MHz.

The aforementioned NIST reference cell has a relatively large footprint due to free space optical components. As lasers and components are made smaller, gas-filled hollow core fibers offer an alternative to current technology. This reference as shown in Fig. 1.1 has been made by free space optics.

Figure 1.1 Fiber coupled acetylene-filled vapor NIST SRM 2517a [7]

With the advent of low loss hollow core photonic bandgap fibers (PBGFs) [8, 9], studies were started on nonlinear and linear spectroscopy such as Raman scattering [10, 11], generation of megawatt optical solitons [12], gas sensing [13], and electromagnetically induced transparency [14, 15] using PBGFs. Due to portability and large interaction of light and gas inside PBGF, it was advantageous to use this optical device as a portable frequency reference [16]. For that, various techniques have been developed to create PMCs depending on the applications.

Over time, different fabrication techniques have been used to seal long PMCs. For example, Triches *et al*. [17] generated a 2.7 m, 0.1 torr optical reference using the encapsulation technique to seal the hollow core fiber. As shown in Fig. 1.2, this novel fabrication technique has 6 steps.

A: A 4-cm-long capillary tube with an inner diameter (ID) is used as a ferrule.

B: The inner diameter of the Capillary is annealed and air is blown to expand the ID.

C: A hole is opened to the larger part of the ID and an external tube will be fused to the capillary tube for future access to the larger portion of the ID.

D: The front facet of the capillary tube is polished and glued to an aspheric lens.

E: The hollow core fiber is then injected to the ID of the capillary and glued. This process happens for both ends of the 2.7m hollow core fiber.

F: The ends are connected to a vacuum pump to evacuate the air, and then the acetylene gas is loaded into the hollow core fiber.

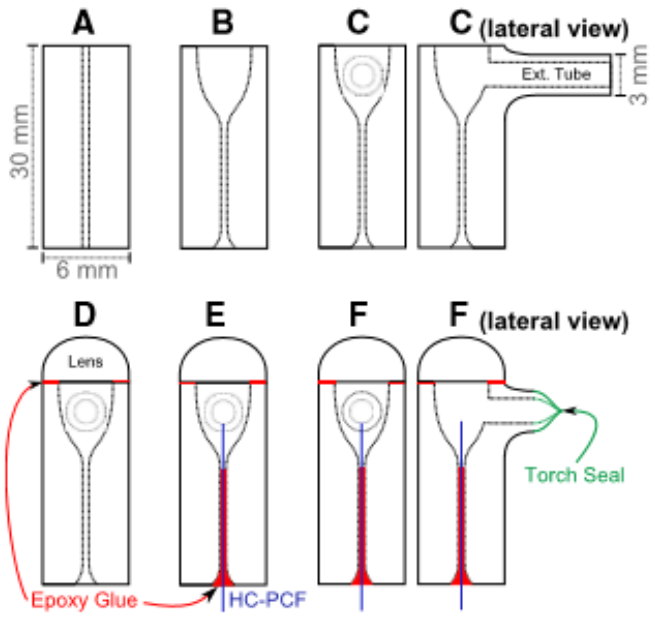

Figure 1.2 Construction of the long PMC using encapsulation technique taken from [17]

In another example, Light *et al.* [18] has made a long PMC by 1m hollow core photonic crystal fiber (HCPCF) initially filled with helium and acetylene with total pressure of between 3750 torr to 7500 torr by using overpressurizing technique. As shown in Fig. 1.3, first, the long 10 μm core PBGF is spliced to a conventional single mode fiber using a filament fusion splicer. Next, it is mounted on a vacuum chamber to purge the PBGF and is loaded with low pressure acetylene gas. The novelty of the technique happens here when PBGF is pressurized with helium. Over pressurizing the PBGF with helium provides enough time to splice the open end of the PBGF to another single mode fiber and trap the acetylene and helium gas inside the PBGF. In the final step, helium gas will diffuse out of the PBGF and the long PMC is ready.

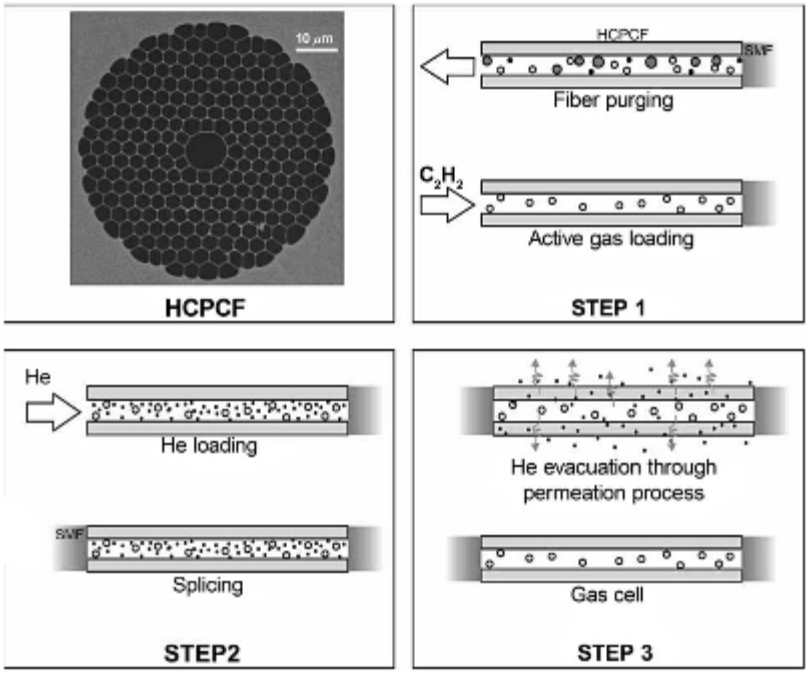

Figure 1.3 Construction of the long PMC using helium overpressurizing technique adapted with permission from [18],[Optics Letter]

Wang *et al*. [19] also created long sealed PMCs based on latter work inside a 1 m acetylene filled PBGF and characterized the accuracy of the PMCs. The aforementioned fabrication techniques are appropriate for long PMCs.

Our goal is to introduce a compact reference with lengths and pressures similar to NIST SRM's, for moderate frequency measurements as described in Luder *et al.* [20]. We will introduce a short, portable, all-fiber, compact reference that has comparable accuracy to NIST SRM 2517a on the line center to calibrate optical devices without the need of free space coupling. This device can be fit into a laser, can be mounted into the photodetectors, and can be connected to multi-mode fibers.

We demonstrate the fabrication using two different methods of sealing short connctorized PMC's called "Q-tipping" and "Tapering''. Thereafter, characterization and results of PMCs like transmission

efficiency, coupling transmission efficiency into multi-mode fibers (MMFs), and the reduction of an etalon-like effect is discussed. As a result, the advantage of using tapering over a Q-tipping technique is specified. While etalon-like effects persist in the tapering method, the cell performance is good enough to satisfy many uses of NIST SRM's. In addition, the total pressure is characterized using Hennigsen *et al.* [21], HITRAN data [22], and Demtroder [1]. Furthermore, the accuracy of the PMC's is checked with the saturated absorption spectroscopy set-up described in Knabe *et al.* [23] and Eq. 1 in Thapa *et al.* [24]. Although connectorization is a well-documented procedure [25], our work [20, 26] introduces it for making short gas-filled PBGF cell references. Since unconnectorized PMCs show a large numeric aperture [20]. connectorization allows two fibers to have physical contact, so light can be coupled directly into MMFs. Finally, long-term stability of a few cells has been measured for the two different methods of fabrication of the PMCs.

Chapter 2 - $v_1 + v_3$ rotational-vibrational band of acetylene gas in near infrared

One of the most important gases that the PMCs are filled with is acetylene gas because it has large number of combination bands between 1510 nm to 1540 nm which covers the telecommunication window [27], and it has been chosen as an international molecular standard [28].

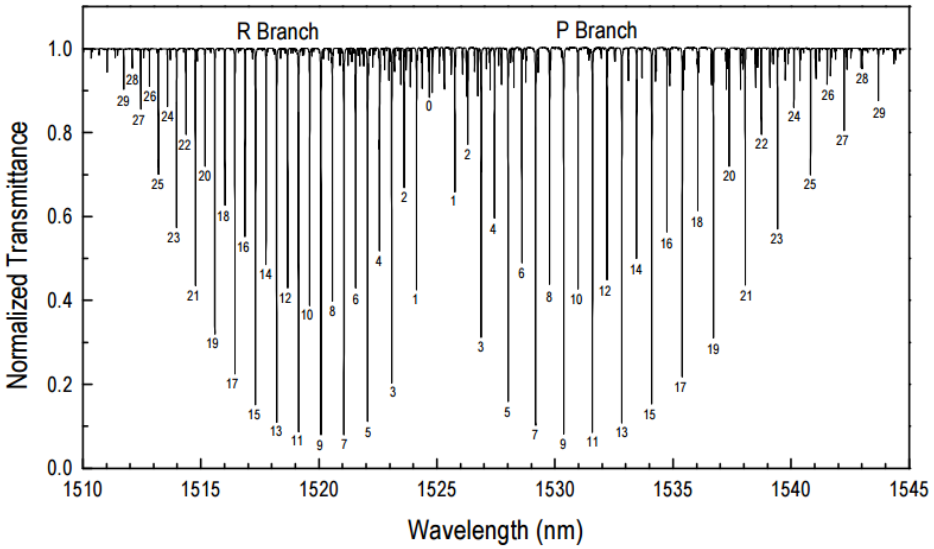

Figure 2.1 Acetylene absorption lines in near infrared taken from [7]

Classically, molecular gas absorbs light because laser light changes the dipole moment of the molecules. Acetylene is a linear polyatomic molecule with seven normal modes of vibration. Only five of these modes have independent frequencies. As shown in Fig. 2.2 among these five modes, only a combination of v_1 and v_3, which is due to the C-H stretching, are active in the near infrared.

Mode	Description	Normal Mode
v_1	Symmetric C-H stretch	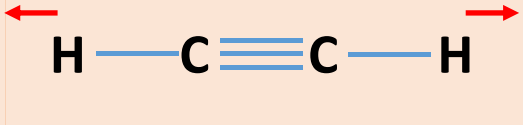
v_2	Symmetric C-C stretch	
v_3	Asymmetric C-H stretch	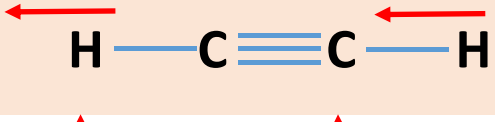
v_4	Symmetric bend	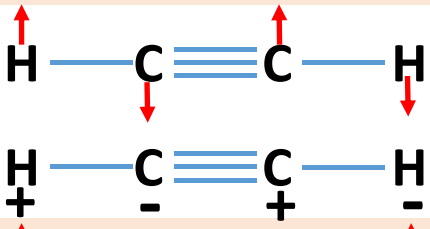
v_5	Asymmetric bend	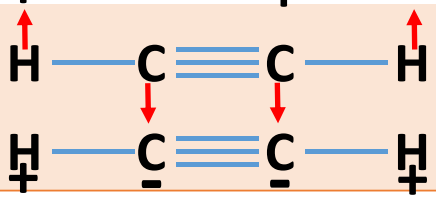

Figure 2.2 Vibrational modes of acetylene inspired by Ref. [29].

Quantum mechanically, there are selection rules for rotational and vibrational transitions among energy states for acetylene gas. Since the light will be absorbed by acetylene gas, selection rule for vibrational energy states happens when $\Delta v=+1$. In addition, because vibrations change the moment of inertia of the acetylene, selection rules of the rotational transitions for acetylene are $\Delta J=-1$ (P branch) and $\Delta J=+1$ (R branch).

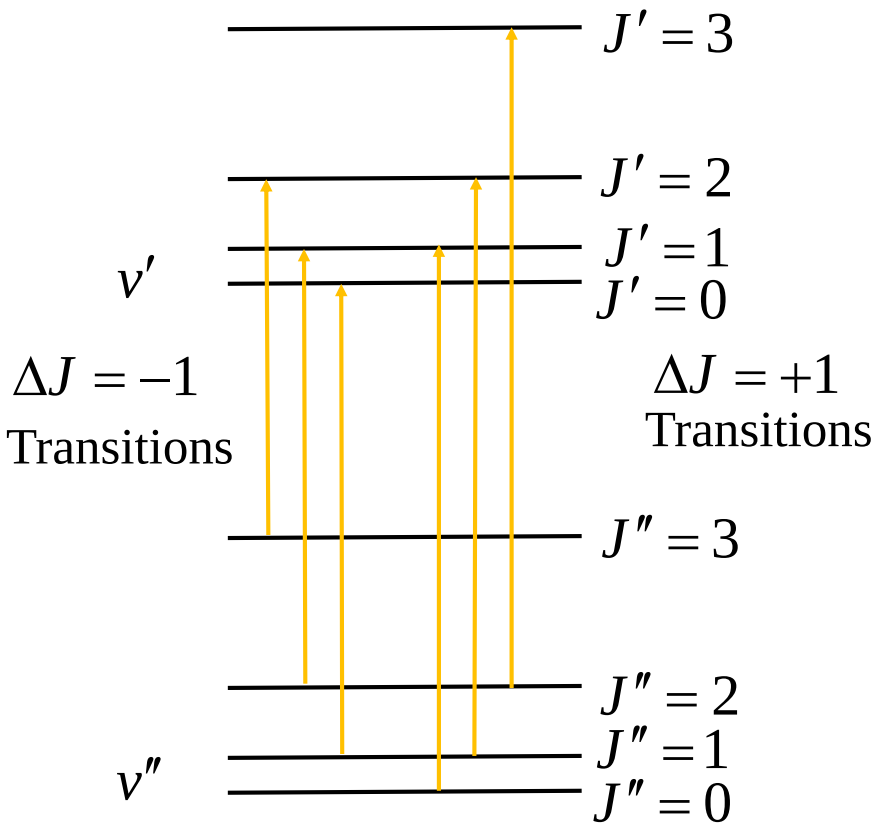

Figure 2.3 Transition lines of acetylene molecule due to the selection rules inspired by Ref. [29].

Among the absorption lines shown in Fig. 2.1, the broadening mechanism of the P13 absorption line is investigated. The peak of the absorption line which has the maximum absorption is called “on-resonance”. With that said the on-resonant point of the P13 line is at approximately 195 THz or 1532 nm. Furthermore, the width of the lines raises from between 500 MHz to 1 GHz.

Chapter 3 - Broadening mechanisms of spectral lines

Line shape functions

The spectra of molecules such as acetylene contain many absorption features called "lines" [30]. The line-shapes are divided into two categories: homogenous and inhomogeneous broadening. Homogenous broadening happens when all the molecules in a system have the identical line-shape profiles. For example, natural lifetime broadening and pressure broadening fall into the homogenous broadening category which are discussed in this chapter. In contrast, inhomogeneous broadening happens when molecules in a system have slightly different absorption spectra. This profile is made up of all the different spectra for the different molecules in the system. For example, Doppler broadening falls into inhomogeneous broadening category as defined in [30] .

Natural lifetime broadening

Absorption or emission spectral lines are not monochromatic as defined in Ref. [1] because energy levels are not infinitely sharp and molecules are moving relative to the observer. The energy levels above the ground state with lifetime of τ_{sp} in principle cannot be distinguished with accuracy better than spontaneous emission. Consider an excited level of E_i with mean lifetime of τ_i and a lower energy state with energy of E_k with mean lifetime of τ_k . The energy E_i can be found with uncertainty of $\Delta E_i = h/2\pi\tau_i$ and as a result, uncertainty of finding E_k is $\Delta E_k = h/2\pi\tau_k$. Consequently, the uncertainties ΔE_i and ΔE_k of the two levels contribute to the linewidth as shown in Eq. (3.1).

$$\Delta E = \Delta E_i + \Delta E_k \rightarrow \delta\omega_n = (1/\tau_i + 1/\tau_k) \tag{3.1}$$

where $\delta\omega_n$ is the uncertainty to find the frequency of transition from E_i to E_k . Figure 3.1 demonstrates the uncertainty principal that relates the natural linewidth to the energy uncertainties of the upper and lower levels.

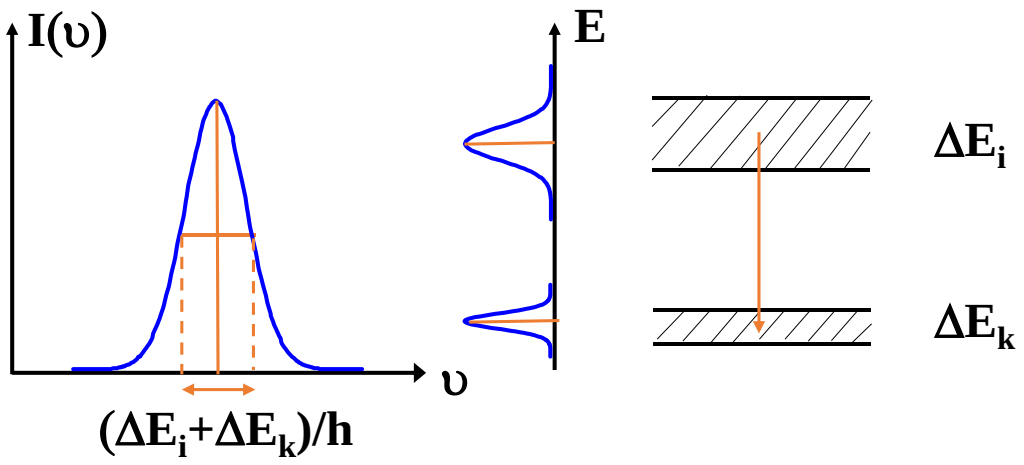

Figure 3.1 Illustration of uncertainty principal for natural linewidth inspired by Ref. [1]

When a weak laser light passes through a sample of molecules the intensity of the laser light changes according to Beer's law as shown in Eq. (3.2).

$$I = I_0 e^{-\alpha(\omega)z} \tag{3.2}$$

Where I_0 is the incident light and $\alpha(\omega)$ is the absorption profile.

In order to find the natural linewidth and absorption line, the semi-classical model of damped harmonic oscillators shown in Eq. (3.3) is used for atoms at rest when charge q is under the influence of a driving force qE and E is the incident laser light of $E=E_0 e^{i\omega t}$.

$$\ddot{x} + \gamma \dot{x} + \omega_0^2 x = \frac{q}{m} E_0 e^{i\omega t} \tag{3.3}$$

Where $\omega_0^2 = \frac{k}{m}$, γ is damping constant, and m is the mass.

Eq. (3.3) has the following steady state solution.

$$x = \frac{qE_0 e^{i\omega t}}{m(\omega_0^2 - \omega^2 + i\gamma\omega)} \tag{3.4}$$

Next, by plugging Eq. (3.4) into the material polarization $P = -Nqx$ and comparing with $P = \varepsilon_0(\varepsilon - 1)E = \varepsilon_0 \chi E$ for acetylene molecules at equilibrium, susceptibility χ of the material as a function of angular frequency is found as shown in Eq. (3.5).

$$\chi = \frac{Nq^2}{m\varepsilon_0(\omega_0^2 - \omega^2 + i\omega\gamma)} \tag{3.5}$$

The relative dielectric constant ε is related to the refractive index n by $n = \varepsilon^{1/2}$. Next, the refractive index can be written as:

$$n^2 = 1 + \frac{Nq^2}{m\varepsilon_0(\omega_0^2 - \omega^2 + i\omega\gamma)} \tag{3.6}$$

Finally, by separating the imaginary and real part of the Eq. (3.6), the frequency dependent absorption coefficient and dispersion for the case of the gases at low pressure is found which is called ***Kramers-Kronig dispersion relation*** as defined in [1] .

$$\alpha(\omega) = \frac{Nq^2\omega_0}{c\varepsilon_0 m} \frac{\gamma\omega}{(\omega_0^2 - \omega^2)^2 + \omega^2\gamma^2} \tag{3.7}$$

$$n'(\omega) = 1 + \frac{Nq^2\omega_0}{2\varepsilon_0 m} \frac{\omega_0^2 - \omega^2}{(\omega_0^2 - \omega^2)^2 + \omega^2\gamma^2} \tag{3.8}$$

The absorption profile $\alpha(\omega)$, which is the imaginary part of the refractive index, is Lorentzian with a FWHM of $\delta\omega_n = \gamma$, which is equal to the natural linewidth and it is less than 5 Hz.

Doppler broadening

When the simple harmonic oscillation equation was solved, we considered that the molecules are at rest, but that is not the case. At low pressures, on the order of mtorr, molecules move with different velocities relative to the rest frame of the observer due to the thermal motion of the molecules. This line-shape is an inhomogeneous type of broadening. At thermal equilibrium molecules of a gas, which is acetylene in our case, follow a Maxwellian velocity distribution [1].

For example, if the z-direction is chosen in a way to coincide with the laser light propagation, molecules that come toward the laser light see the laser light blue-shifted and for the case of molecules moving away, they see the laser light red-shifted. For that, frequency dependent intensity profile is represented by a Gaussian profile as shown in Eq. (3.9)

$$I(\omega) = I_0 \exp(-\frac{(\omega-\omega_0)^2}{0.36\delta\omega_D^2}) \tag{3.9}$$

where $\delta\omega_D$ is the Doppler width which increases linearly with the frequency ω_0.

This broadening at low pressure is called “Doppler broadening”. The Doppler width is a constant value of 474 MHz for the case of the acetylene gas at room temperature and molecular mass of 26 amu. The Doppler width in frequency units is given by the following Equation:

$$\delta\nu_D = 7.16\times10^{-7}\nu_0\sqrt{\frac{T}{M}} \qquad [Hz] \tag{3.10}$$

Where T is the room temperature, and M is the acetylene molecular mass.

Pressure broadening

At high pressures on the order of torr, not only there is Doppler broadening, but also there is another type of broadening due to the interaction of the molecules. Additionally, at high pressures Doppler broadened line cannot be represented by a pure Gaussian. Because of the finite life times of the molecular energy levels, the frequency response of these molecules is accompanied by Lorentzian profiles as well as shown in Eq. (3.11).

$$L(\omega) = \frac{1}{\pi} \frac{\Gamma}{\omega^2 + \Gamma^2} \tag{3.11}$$

Where, $\Gamma = \gamma/2$ is half of the Full width at half maximum (FWHM).

Due to molecular interactions, the natural line width of the molecules becomes broader and the center of the profile shifts to lower frequencies. For example, for P13 line center of acetylene that is at 1532 nm or 195 THz, for a pure cell filled with 50 torr acetylene this shift factor is -0.3 MHz/torr where the minus sign indicates a shift to lower frequency.

Voigt profile

Now that there are two types of dominant broadening happening at high pressures, which broadening represents the intensity profile? Is it a Gaussian profile or a Lorentzian profile?

And the answer is the intensity profile is represented by a convolution of a Gaussian and a Lorentzian profile which gives Voigt profile as shown in Eq. (3.12).

$$V(\omega) = L(\omega) \otimes G(\omega) \tag{3.12}$$

Basically, by comparing the Gaussian profile with a Lorentzian profile with equal half widths, Gaussian profile drops fast on the sides of its profile which are called “wings” while the Lorentzian drops fast in the middle part of its profile which is called “kernel”.

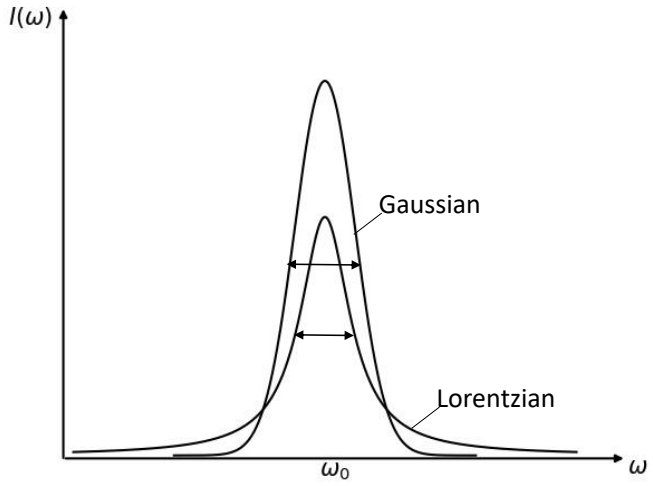

Figure 3.2 Comparison between a Gaussian and a Lorentzian profile inspired by Ref. [1]

Voigt profile takes into account both contributions of the wings and kernel. As Fig. 3.3 shows in the case of the Voigt profile, kernel is dominated by the Gaussian profile and wings reflect the contribution of the Lorentzian profile.

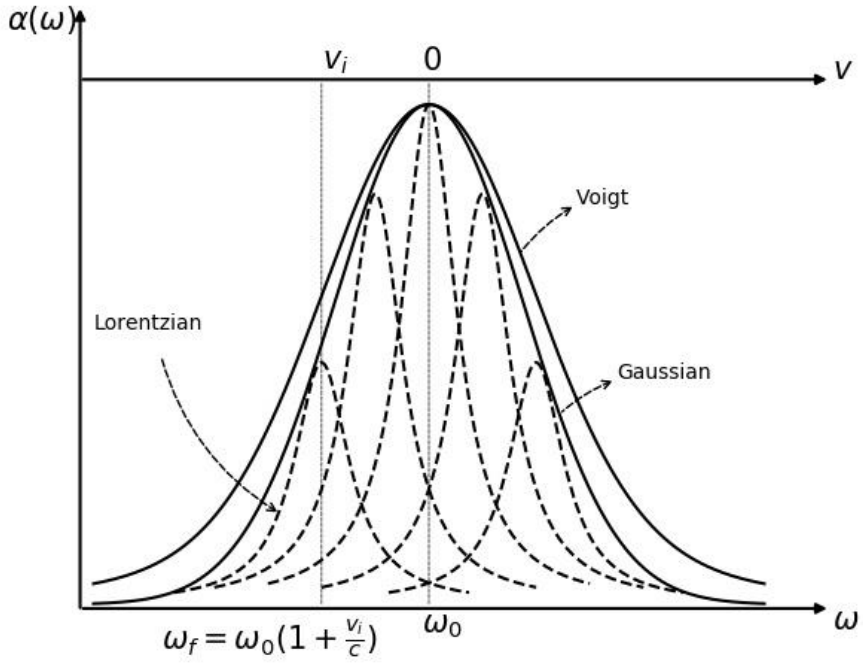

Figure 3.3 Voigt Profile as a convolution of a Lorentizan and a Gaussian profile inspired by Ref. [1].

Another interpretation of the Voigt profile is that there is only one Gaussian profile due to thermal motion of the molecules, but molecules have different frequency responses due to their different life-time, so there are many Lorentzian profiles under a Gaussian profile. Therefore, each one of the Lorentzian profiles is scanned under the Gaussian and finally one gets a convolution of those profiles as a Voigt profile.

Chapter 4 - Photonic bandgap fiber (PBGF)

To develop a fiber-based optical reference that depends on molecular absorption, a hollow core photonic crystal fiber (HCPCF) is necessary. One option is using capillary fibers. Because the core has a lower index of refraction than the surrounding fused silica cladding, the guidance happens through reflection and the process is lossy. For example, the loss for the capillary of 100 μm core at 1500 nm is 5 dB/m and should be oriented carefully, as small bends can greatly increase the transmission loss. On the other hand, low loss hollow core photonic crystal fibers offer guidance similar to that of single-mode fibers of 10^{-2} dB/m. Moreover, they are capable of being filled with gas. For comparison, single-mode fiber is one of the main fibers used in the telecommunication network due to its low optical transmission loss of 0.2×10^{-3} dB/m. It is all solid and made of fused silica. This fiber experiences guidance by means of total internal reflection due to the core having a slightly higher refractive index than the surrounding silica cladding. The core has a diameter of 9 μm and the cladding diameter is 125 μm.

Now let us go back to the PBGF. As it was mentioned, there is a class of HC-PCF called photonic bandgap fibers for which transmission loss is low [8, 9] and that guides light due to the photonic bandgap effect. To have a better idea of light guidance in PBGFs, let us look at Fiber Bragg gratings (FBG). As shown in Fig. 4.1, a FBG is a 1-D photonic crystal (or better say it has 1-D periodic structure) that consists of two alternating layers of different materials that have different refractive indices. It reflects certain optical frequencies (f_R) due to this structure and transmits all other frequencies (f_T) [31].

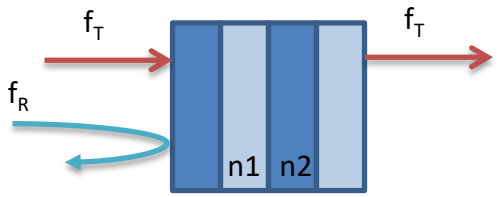

Figure 4.1 Bragg grating structure: a one-dimensional photonic crystal

In case of PBGF as shown in Fig. 4.2, it has a periodic array of air holes or two-dimensional photonic crystal lattice surrounding a hollow core of 20 μm that causes destructive interference in the cladding, but not in the core. In our case the hole core and the spacing among the periodic array of air-holes are optimized in such a way that the fiber guides light at 1550 nm with a bandwidth of 200 nm.

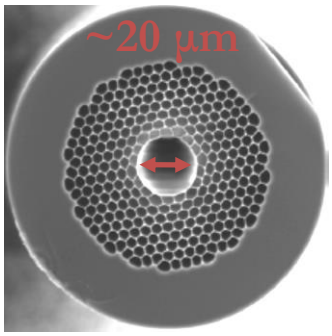

Figure 4.2 HC19-1550 PBGF, NKT Photonics

An important tool for analysis of periodic structures is the photonic band diagram. The Band diagram reveals the frequency intervals in which no mode solutions are found. Therefore, no modes at such frequencies will be able to propagate throughout the structure. Figure 4.3 shows the band diagram of the PBGF for different wave vectors of kΛ.

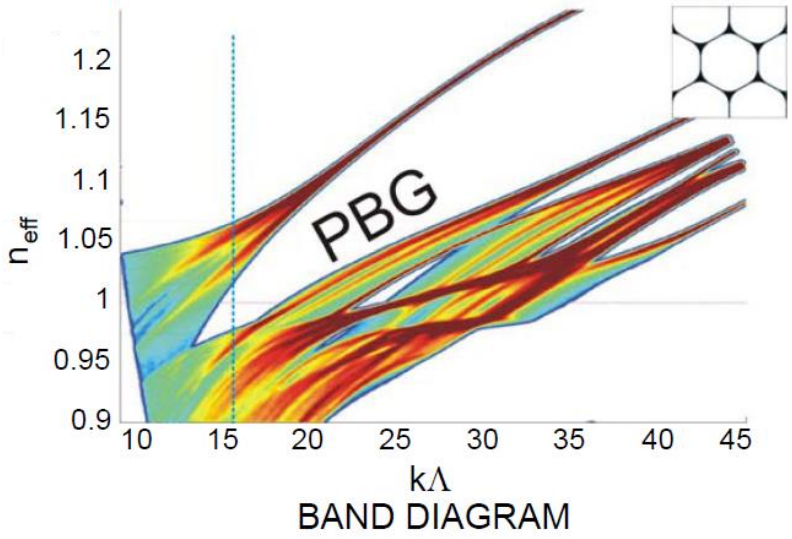

Figure 4.3 Band diagram showing the presence of photonic bandgap effect taken from [32] with proper acknowledgment as given on page 59.

Chapter 5 - Construction of short photonic microcell and applications

Construction of the PMC includes four steps; (1) splicing the 20 μm core PBGF (HC19-1550) to a telecommunication grade single mode fiber (SMF) (SMF28E) as shown in Fig. 5.1(a), (2) placing the open end of the PBGF into a vacuum set-up, evacuating and filling the fiber with acetylene gas, (3) tapering or Q-tipping the fiber to seal the PMC, and (4) connectorization of the PMC. As shown in Fig. 5.1(b) and Fig. 5.1(c), on the left-hand side of the figures is a needle that is created during the process of Q-tipping or tapering the core and cladding.The right end shows the fabrication method of Q-tipping in Fig. 5.1(b) and tapering in Fig. 5.1(c).

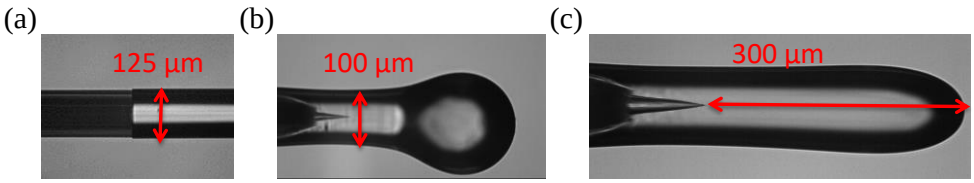

Figure 5.1 (a) Camera images of the splice between 20 μm core PBGF (HC19-1550 Thorlabs) on the left-hand side and SMF (SMF28E) on the right-hand side. (b) Camera image showing the collapsed cell end of PBGF. (c) Camera image showing the tapered end of PBGF.

Splicing the PBGF to SMF

The first step towards making a PMC is splicing an approximately 1 m length of PBGF to a SMF using a Vytran filament fusion splicing system [FFS-2000]. The PBGF is commercially available and is chosen such that we can achieve appreciable mode matching to other fibers.

The splicer is calibrated with a normalization routine and then the splicing program with splice parameters shown in Table 5.1 is applied to splice the SMF and PBGF interface giving us a half-cell. Figure 1(a) shows an image of the splice taken using the splicer camera. A protection

sleeve is melted on the splice of SMF to PBGF to protect the splice. The quality of the splice is tested by measuring its transmission. We have been able to achieve typical transmission of approximately 90% and up to a maximum of 95% using the splice program in Table 5.1.

Table 5.1 Splice parameters for PBGF20 to SMF28 splice

Splice parameters	**Value**
Pre-gap (μm)	8.0
Pre-push (μm)	8.0
Hot push (μm)	6.0
Hot push delay (s)	0.35
Argon (min-1)	0.65
Push velocity (μm /s)	86
On duration	1.05
Power (W)	15.00
Splice offset (μm)	100

Evacuating the spliced fibers and filling with acetylene

The open end of the half-cell is attached to a vacuum chamber with a custom-made feed-through and evacuated to mtorr levels for approximately 24 hours using both roughing and turbo pumps. The chamber is evacuated for a day and the setup is filled with acetylene at a given pressure for an hour. In our case, the acetylene pressure in the vacuum chamber varies from 7.3 – 80 torr. Next, P13 or P11 absorption lines of acetylene are being checked while the system reaches equilibrium, as is evident from the stability of the absorption line. The vacuum chamber is attached to a capacitance manometer [MKS instruments XDCR500T2-¾-CFROT 0.25%] that gives the pressure readout. Having that said, cells are made for different combinations of length and pressure.

“Tapering” or “Q-tipping” the open end of PBGF

Next step in making the PMC is sealing the open end of the PBGF. This can be done by using two different methods: tapering or Q-tipping. The end of PBGF can be Q-tipped while having acetylene gas trapped inside of it. Specifically, about one inch of the PBGF fiber is stripped using a razor blade and inserted into the arc fusion splicer. A brief pulse of current causes the PBGF fiber to collapse and a ball of glass to form, sealing acetylene inside the PMC as shown in Fig. 5.1(b). Or, it also can be sealed by the tapering method. During the process of tapering, the splicer simultaneously pulls and heats the PBGF into an hour glass shape that finally separates the PBGF as shown in Fig. 5.1(c). For that, the Ericsson fusion splicer (FSU 995FA) is used with the settings shown in Tables 5.2 and 5.3 for these processes.

The recipe for Q-tipping the PBGF is executed by built-in program 1 (normal SM+SM) of the splicer. This program splices two single mode fibers. In this program fusion currents are optimized such that a Q-tip forms on the end of the PBGF. In this program fusion current 2 is increased from 16.3 mA to 20 mA to allow the process of separating and sealing the PBGF to be completed. The process of Q-tipping takes about 3 to 4 seconds and depends on the pressure to which the PBGF is filled with acetylene.

The recipe for tapering the fiber is extracted from program 9 (SM fiber lens). This program tapers a single mode fiber. In addition, it is optimized to taper the PBGF. It consists of three rounds of pulling, and each is associated with the fusion current and fusion time. To apply the process of tapering for PBGF, just the first round of pulling (Pull 1) is used. Furthermore, the fusion time 1 is user determined and is manually stopped when the process of sealing the PBGF is done. The process of tapering PBGF takes about 5-8 seconds and it depends on the pressure to which the PBGF is filled with acetylene.

Table 5.2 Recipe for Q-tipping the open end of PBGF

Splice parameters	Value
Prefuse time (s)	0.2
Prefuse current (mA)	10.0
Gap (μm)	50.0
Overlap (μm)	10.0
Fusion time 1 (s)	00.3
Fusion current 1 (mA)	13.0
Fusion time 2 (s)	2.0
Fusion curent 2 (mA)	20.0
Fusion time 3 (s)	2.0
Fusion curent 3 (mA)	12.5
Left MFD (μm)	9.8
Right MFD (μm)	9.8
Set center	+255
AOA current (mA)	0
Early prefuse	No
Align accuracy (μm)	+0.15
Loss shift (dB)	0
Auto arc center	No

Table 5.3 Recipe for tapering the open end of PBGF

Splice parameters	Value
Fusion current 1	15 mA
Fusion time 1	5-8 sec
Pull 1	Yes

Connectorization

The final step in making the PMC is connectorization. Because light exits the fiber in a cone-shaped spatial pattern, coupling into or splicing to a single-mode fiber after collapse has

proven lossy as described in [8]. Our solution is to connectorize the bare fiber ends, so the PMC light can be coupled directly onto a photodetector, and can be physically contacted to multimode fibers.

Two different processes are developed for connectorizing PMCs. For the first method (called the “Tapering Method”), the fiber ends are tapered, placed in a connector and polished as similarly done with any type of step-index fiber. First the epoxy (Thorlabs F112, 24 hr. cure time) is injected into the ferrule. Second, the PMC tip is fitted into a 126 μm standard FC/PC connector (FIS F12070900). Third, the cell tip is scribed 150 μm away from the needle of the tapered cell as shown in Fig. 1(c) under the microscope. When the epoxy is cured, the cell tip is polished. Since the width of the tapered cell is approximately 100 μm, it fits into the standard FC/PC connectors. Standard connectorization of the very short tapered cells are easier and make them more robust inside the connector. With that said, we are able to make a connectorized tapered cell with 12% transmission to the large area detector with absorption of 25%.

Q-tipped PMC is also polished and connectorized by a method called the “Q-tipped Method”. For a Q-tipped PMC, the tip is inserted into a custom-drilled connector (FIS F12772190) which extends 300 μm from the ferrule. Then the epoxy (Thorlabs F112, 24 hr cure time) is injected into the connector and fills the connector. The epoxy does not cover the tip of the Q-tipped cell and ferrule. Next, the tip of the PMC is pulled back until the ferrule end and tip are even. After the epoxy is cured the ferrule is cleaned and no polishing is needed. The best off-resonant transmission achieved using Q-tipped connectorization is 4%.

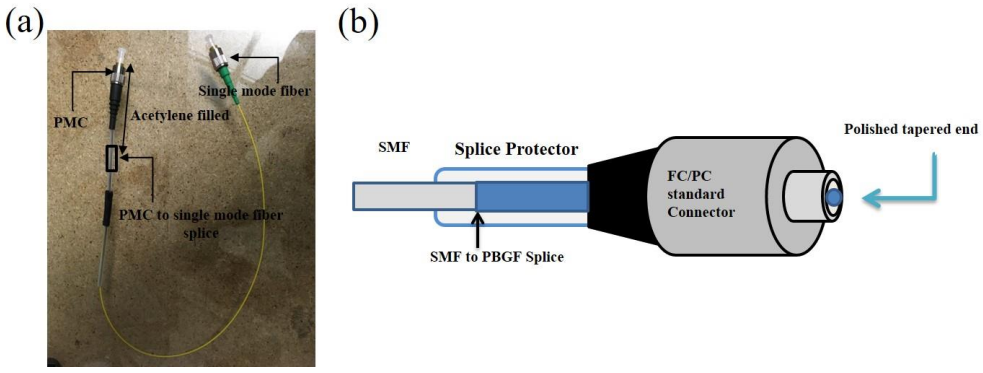

Figure 5.2 (a) Picture of the connectorized tapered PMC no. 53 (b) Schematic of a connectorized PBGF tapered cell.

PMC application

As Fig. 5.3 shows, the PMC can be fit into a tunable laser source and can be used to calibrate it. For that, the PBGF end of the PMC needs to be connected to a large core multimode fiber such as 400 μm core MMF, and the MMF is connected to a large area detector. Consequently, by tuning the laser source across the maximum absorption on the detector, one could calibrate the tunable laser source. It is not necessary to fit the PMC into the laser device. For such a case, the PMC can be directly connected to the large area detector.

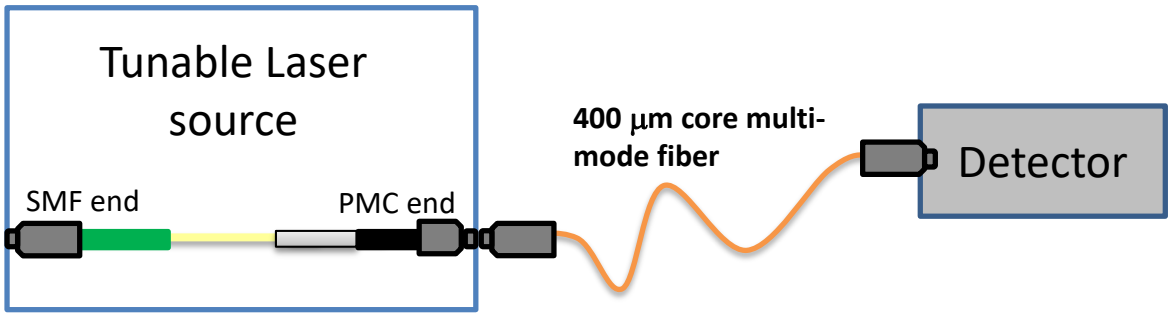

Figure 5.3 PMC application: The schematic shows a PMC fitted into a tunable laser source. The collapsed PBGF end is connected to a 400 μm core MMF and the MMF is connected to a large area detector.

Chapter 6 - Characterization of the photonic microcell

Transmission, absorption, and coupling measurements

One challenge in creating a PMC is achieving high optical transmission efficiency while trapping gas. PMC transmission was measured when the laser was off-resonant with absorption lines of acetylene gas. The PMC absorption was measured with respect to the P13 absorption line at 1.53 μm.

The transmission of the PMC is given by the ratio of power incident on SMF input to the power output at the tapered or Q-tipped end of the PMC. This also includes SMF-PBGF splice loss and taper or Q-tip loss.

In order to measure absorption, the laser frequency was swept across the P13 absorption line of acetylene and the ratio of the power on-resonance to the power off-resonance was measured at the output of the PMC. The best tapered PMC transmission was 82% with absorption of 50%. The PMC length was 10 cm and the vacuum set-up was filled to an acetylene pressure of 36 torr.

One of the reasons that we changed to the tapering method was that the Q-tipping method had a lower off-resonant transmission compared to the tapering method. The best off-resonant transmission achieved by Q-tipped cells was 37%, which is a factor of two smaller than the best tapered cell off-resonant transmission.

Transmission efficiency of the PMC was determined by measuring the transmission through butt-coupled 400 μm, 200 μm, and 62.5 μm core multimode fibers. The experimental setup shown in Fig. 6.1 is used to measure this parameter where the unconnectorized PMC is butt- coupled with MMF by careful manual alignment in the Ericsson fusion splicer. The light from a tunable fiber-coupled diode laser near 1.53 μm is coupled into the SMF patch cable part of the PMC which has an FC/APC connector. When the cell contains acetylene, care is taken to tune the laser off-resonance to avoid significant cell

absorption. As shown in Fig. 6.1, the power measured out of the SMF patch cable is recorded as power level A, and can be re-measured throughout the process. A large-area photodetector with Germanium semiconductor inside it is brought as close as possible to the tapered end to record the transmitted power B, and tapered cell transmission is B/A. Finally, light is coupled from the cell into an MMF, and the transmitted power is measured at C, making the transmission efficiency of the cell into MMF equal to C/B.

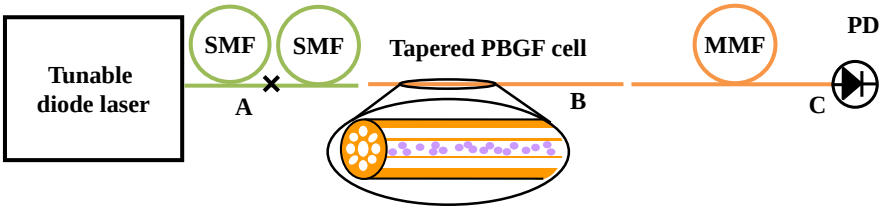

Figure 6.1 Power measurements used to characterize cell transmission efficiency. A: power measured out of fiber-coupled laser source. B: Power measured after collapsing fiber cell. C: Power measured through 400 μm [BFL48-400 THORLABS] and 200 μm [FT200EMT THORLABS] core multimode fibers (MMF). All power measurements are made off-resonance in the case of acetylene-filled cells. The laser wavelength is approximately 1532 nm.

Our goal for butt coupling the PMC to MMF was to check whether it was possible to get a noticeable transmission before connectorization through multimode fibers or not. Table 6.1 shows the optimized coupling transmission through MMFs. In addition, Table 6.1 gives the measured fractional transmission through two different tapered PMCs. We report results for PMCs no. 52 and 53 with length of 6 cm, and fractional absorption of 25%.

Table 6.1 Butt coupling transmission for 20 μm tapered, unconnectorized cells no. 52 and 53.

PMC no.	Splice transmission	Cell transmission (B/A)	400 μm core MMF (C/B)	200 μm core MMF (C/B)	62.5 μm core MMF (C/B)
53	93%	78%	61%	52%	2%
52	94%	80%	61%	41%	3%

Pressure broadening and acetylene pressure measurements

To characterize the gas purity and pressure, we examine the pressure broadening and integrated optical depth, and deduce partial pressures of acetylene and air, for each PMC.

Set-up schematic

To carefully measure absorption of the cells, a tunable laser is coupled into PMCs and scanned across the feature, as shown in Fig. 6.2, the ring cavity transmission, cell absorption line, and signal generator data are simultaneously taken using two Red Pitayas as data acquisition (DAQ). Ring cavity output, used for frequency calibration, is integrated with the large area detector (IR photoreceiver new focus). The connectorized PMC is connected to the large area detector (IR photoreceiver new focus). Photodetectors are connected to DAQs and the signal generator is directly connected to the DAQ no. 1 to which photodetector no. 2 is connected. Both DAQs are synced to take data at the same time.

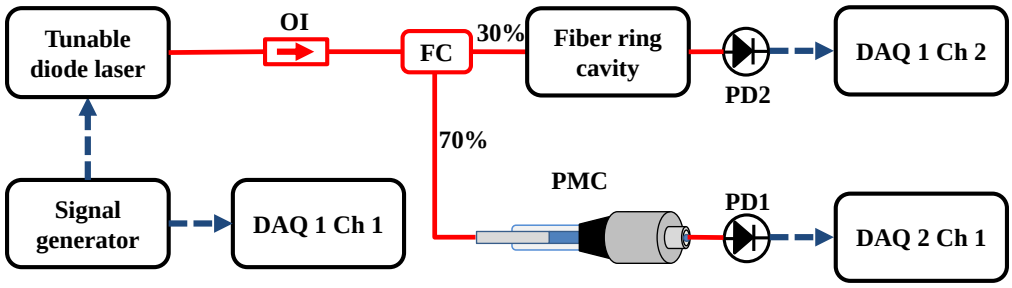

Figure 6.2 Schematic for characterizing the pressure inside PMCs: Diode laser [SANTEC tunable semiconductor laser TSL-210] works in the 1.5 μm range, ring cavity for frequency calibration, PD1 and PD2 are large area detectors [IR photoreceiver] for inspecting the ring cavity transmission and PMC P13 absorption line, two Red Pitayas are used as DAQs, signal generator and Ring cavity transmission to photo detector no. 2 are connected to DAQ no. 1 channels 1 and 2. PMC absorption. FC is a 30%- 70% fiber coupled beam splitter, OI is an optical isolator, and Blue dashed lines are electrical signals.

Figure 6.3 shows the processed data, taken by a 14 bit Red Pitaya interface used as a DAQ. This data set shows tapered cell no. 48 absorption to PD1, ring cavity output transmission to PD2, which is used for finding relative frequencies, and the sweep of the ramp voltage is taken by DAQ 1 channel 1. In Fig. 6.3 the ramp voltage sweeps from low to high frequencies. The x axis frequency was calculated with respect to the P13 line frequency.

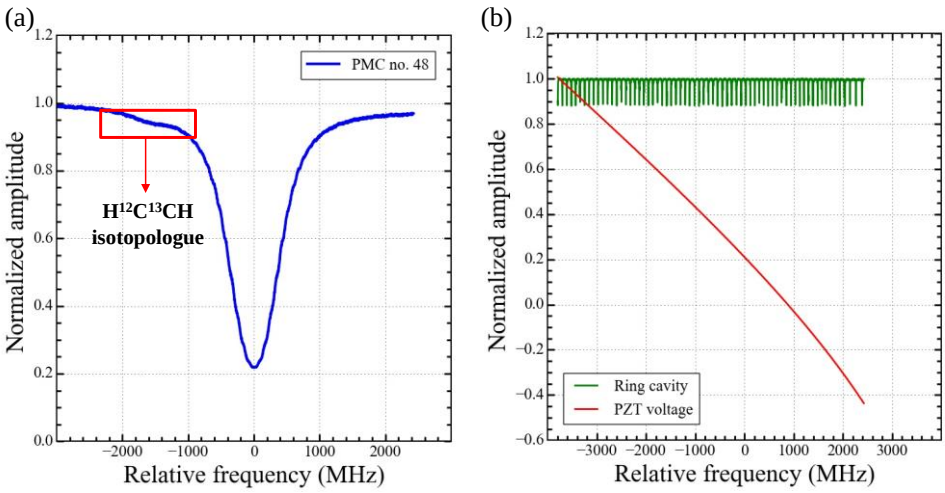

Figure 6.3 (a) Calibrated transmittance for PMC no. 48 derived by PD 1 in Fig. 3. The bump on the left side of the P13 line shows the $H^{12}C^{13}CH$ absorption line (2nd isotopologue of acetylene) approximately1500 MHz away from P13 line. (b) Calibrated data for ramp voltage derived from DAQ 1 Ch 1 which is used to drive PZT of tunable laser and ring cavity transmission derived from PD 2 with free spectral range (FSR)=93 ± 1 MHz.

Fitting models

From the measured absorption line, Beer's law $I = I_0\, e^{-\alpha(\nu)L}$ is used to calculate frequency dependent optical depth, $\alpha(\nu)L$. In order to find the pressure broadening, optical depth is fit to a Voigt profile using a Python fitting module called lmfit [33]. As mentioned before, the intensity profile is a Voigt profile, which is a convolution of Gaussian, due to Doppler broadening, and a Lorentzian, due to pressure broadening [1]. The Gaussian FWHM is 2.35σ in the fitting code, and Γ is the Lorentzian HWHM in the fitting code. For fitting the data to a Voigt profile, σ is fixed to 201.4 MHz in the code for the case of acetylene gas at room temperature [1].

Once the Gaussian FWHM is fixed, then the optical depth is fit to a Voigt profile and a best-fit value is obtained for Γ. To extract the pressure from the measured pressure broadening for a case of a pure cell that is filled only with acetylene, the Lorentzian FWHM 2Γ is found in the first step. Then, the pressure is found by dividing the Lorentzian FWHM by the pressure broadening factor for the P13 line extracted from Swann *et al.* [7]. According to NIST's extensive studies on acetylene broadening in these pressure regions, the collisional or pressure broadening parameter is 11.4 MHz/torr for P13 line [7]. The process of finding the pressure can be done for different acetylene lines using the pressure broadening parameter and Lorentzian FWHM of that certain line. Figure 6.4 shows fitted optical depth to the Voigt profile for PMC no. 53. The difference between the optical depth and the fitting of cell no. 53 is shown as residuals in Fig. 6.4.

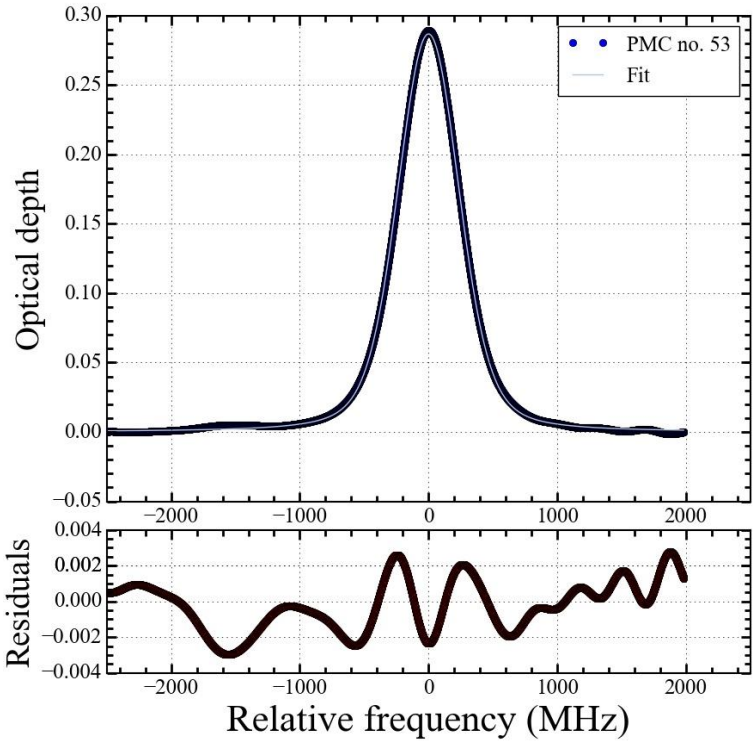

Figure 6.4 PMC no. 53 fitted to the Voigt profile to find the pressure broadening with residuals.

Measuring partial pressures

From the calculated $\alpha(\nu)L$, the partial pressures of acetylene and air contaminant are determined. First, acetylene partial pressure or pressure of absorber is calculated by integrating $\alpha(\nu)L$. Next, the air contaminant is found from the pressure broadened width plot of $\alpha(\nu)L$ versus frequency.

The HITRAN data for P13 acetylene line strength [22], and the relationship between the optical depth and the pressure of the ideal gas due to acetylene is used to find the acetylene pressure. Then the absorption coefficient is given by Eq. (6.1).

$$\alpha(\nu) = nSG(\nu - \nu_0) \tag{6.1}$$

where n is the number of molecules per unit volume, S is the HITRAN line strength of the chosen acetylene absorption line 31.01×10^{-11} Hz/(molecule cm^{-2}) for P13, and $G(\nu-\nu_0)$ is the area normalized line shape function which is a Voigt profile for this case. Since the pressure of acetylene is just an unknown parameter, acetylene partial pressure can be derived from the area A under the absorption profile.

$$A=\int_0^{\infty}\alpha(\nu)L\,d\nu=\int_0^{\infty}\frac{P_a L}{kT}S\,G(\nu-\nu_0)\,d\nu \tag{6.2}$$

$$P_a=\frac{AkT}{LS} \tag{6.3}$$

On the left-hand side of Eq. (6.2) is the integration of the optical depth in the frequency domain and gives the area of the optical depth. On the right hand-side $\int_0^{\infty}G(\nu-\nu_0)\,d\nu=1$ is an area normalized function. In Eq. (6.2) and Eq. (6.3), k is the Boltzmann constant and T is the room temperature.

Having the acetylene partial pressure P_a from Eq. (6.3) and the Lorentzian HWHM Γ determined from the Voigt fit, the air partial pressure can be determined using the equation $\Gamma=\gamma_c P_c+\gamma_a P_a$ where γ_c is the contaminant broadening factor, P_c is the contaminant partial pressure, and γ_a is the acetylene broadening factor. HITRAN values for broadening factors are γ_a=5.6 MHz/torr and γ_c=3.07 MHz/torr [22].

Result for PMC no. 53 and half-cell A

By Voigt fitting of Fig. 6.4 and analysis of previous subsection, the Lorentzian HWHM Γ, pressure of absorber P_a , and contaminant pressure P_c were found for connectorized tapered PMC no. 53 as shown in Table 6.2. Before sealing PMC no. 53, the vacuum set-up was filled to 12 torr with acetylene. The same analysis was done as a comparison for a half-cell, which is a PBGF with one end spliced to SMF and the open end attached to a vacuum chamber with a custom-made feed-through. The half-cell was filled to the chosen acetylene pressure, and the following parameters in Table 6.2 were found for half-cell A, when the vacuum set-up was filled to 14 torr.

Table 6.2 Charactarization of PMC no. 53 unconnectorized tapered cell.

PMC no.	transmission	Length	$P_a(C_2H_2)$	P_c(air)
53	78%	6 cm	3.1 torr	15 torr
Half-cell A	93%	40 cm	13.9 torr	0 torr

Comparing measured absorption for PBGF half-cell and a PMC to SpectralCalc

To verify the partial pressures found above, the frequency dependent optical depth computed using SpectralCalc for values from Table 6.2 for PMC no. 53 and half-cell A. SpectralCalc is a software package [34] that computes the optical depth of the gas cells for the chosen length, temperature and partial pressures based on assumed line shapes and HITRAN data. The found optical depths were consistent with Table 6.2.

We verified using SpectralCalc that the measured optical depth spectra are inconsistent with an uncontaminated PMC. In other words, partial pressure measurements done for half-cell A show that no air contamination was introduced to the set-up when the half-cell was held in the vacuum set-up filled with acetylene.

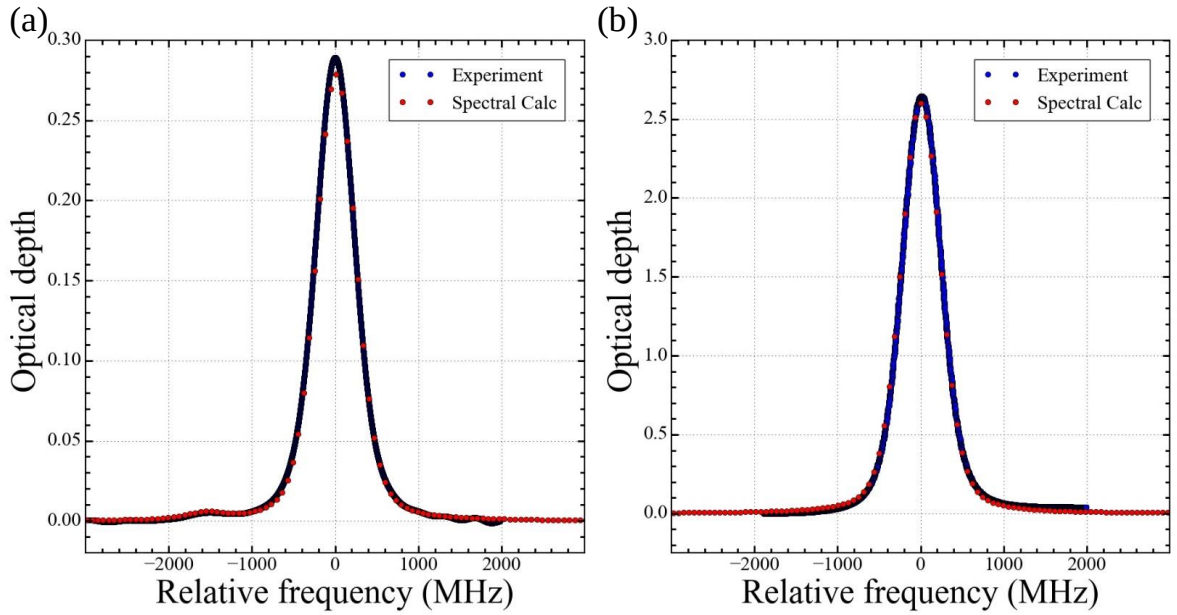

Figure 6.5 (a) SpectralCalc P13 line comparison plot with experimental data for PMC no. 53 with total pressure of 23 torr and temperature of 296 k. (b) SpectralCalc P14 line comparison plot with experimental data for 40 cm half-cell A with total pressure of 18.85 mbarr (14.1 torr), pure acetylene and temperature of 296 k.

Contamination characterization

Contamination was measured for another half-cell B and subsequently two PMCs made from it by Q-tipping and re-Q-tipping it. The half-cell B was uncontaminated, while the Q-tipped PMCs showed some contamination according to Table 6.3. When PMC no. 58 is made from half-cell B, the acetylene partial pressure decreased from 9.4 torr to 7.7 torr. Similarly, when PMC no. 59 was made from PMC 58, the pressure decreased to 5.7 torr while contamination pressure increased. As shown in Table 6.3 we verified that due to some unknown physical process air appears to leak into the PMC each time it is collapsed, while the acetylene partial pressure simultaneously decreases.

Table 6.3 The partial pressure in the photonic crystal fiber before (half-cell) and after collapse. Cell no. 59 was made by collapsing cell no. 58 a second time, making it shorter.

Cell no.	Length	P_a (C_2H_2)	P_c (air)	P_{total}	Γ	Contamination
Half-cell B	56.0 cm	9.4 torr	0.0 torr	9.4 torr	52.0 MHz	0.0 %
58	23.0 cm	7.7 torr	7.2 torr	14.9 torr	66.2 MHz	48.5 %
59	10.5 cm	5.7 torr	15.0 torr	20.7 torr	78.6 MHz	72.5 %

Accuracy

The center wavelength of the pressure-broadened feature for connectorized, tapered PMC no. 53 was measured to compare with the description of NIST SRM 2517a in Ref. [1]. The set-up shown in Fig. 6.2 was integrated with sub-Doppler gas-filled HC-PCF described in Knabe *et al.* [23]. The center of the subDoppler feature was found to 10 kHz accuracy [23]. Then the PMC optical depth was recorded simultaneously with the sub-Doppler feature for six sets of data for the same cell no. 53. The sub-Doppler reference (fiber length 4.5 m) was filled with 170 mtorr, while cell pressure was on the order of torr. The sub-Doppler feature was shifted from the center of the Doppler because the probe was shifted by 55 MHz from pump using an acousto-optical modulator (AOM) to decrease the noise due to pump and probe interference. The sub-Doppler optical depth was fit to Eq. (2) of Ref. [24] while the PMC was fit to a Voigt profile. The frequency separation between the sub-Doppler and PMC varied by less than 10 MHz for six sets of data. Figure 6.6 shows the experimental data taken for the small shift between the sub-Doppler and cell center. The maximum value of shift separation between sub-Doppler and cell center for six sets of data for the same cell was 15.4 ± 3.3 MHz. Although the cell is highly contaminated, experimental data shows that this separation is small.

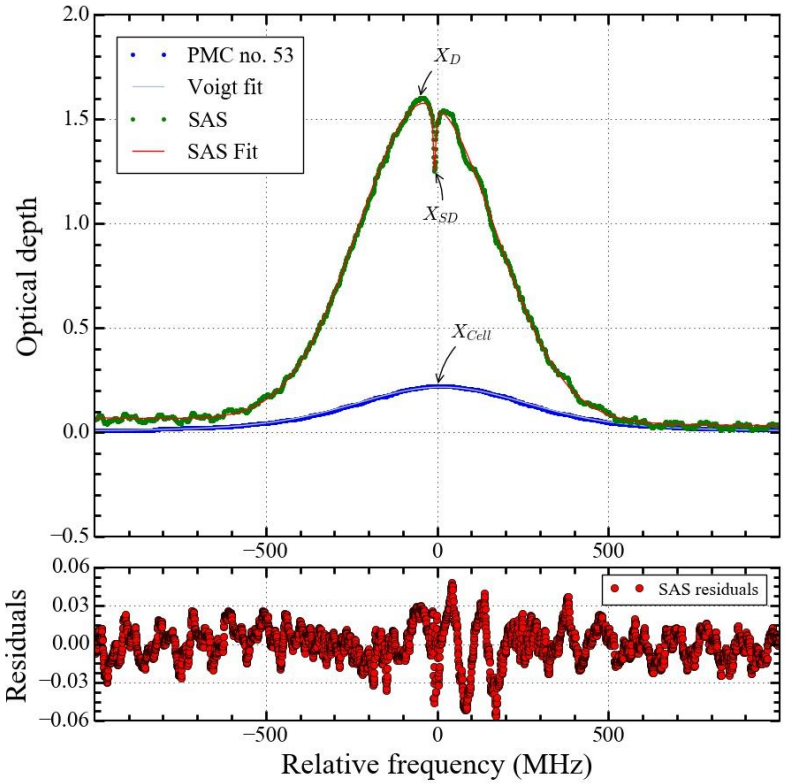

Figure 6.6. Comparison of Saturated absorption spectroscopy reference simultaneously with optical depth of connectorized PMC no. 53 accompanied by SAS residuals. X_{Cell} is center of the PMC P13 line, X_{SD} is the center of the sub-Doppler and X_D is the center of the Doppler. The solid red lines show the fittings to sub-Doppler and cell center.

Etalon-like effects

Errors in the line center are due to multi path interference observed as an etalon-like effect [26]. Due to this etalon-like effect, Q-tipped cells show amplitude and frequency modulations on the wings of the absorption line. This modulation is greatly reduced for tapered cells than for the Q-tipped cells as shown in Fig. 6.7. The Q-tipped cell exhibits an etalon-like modulation in the transmitted intensity with two components. The largest amplitude of 13% has a frequency of 2 GHz, while a smaller amplitude of approximately 2% is observed with a 25 MHz frequency.

We were able to eliminate the 2 GHz modulation by using the tapering technique, but 25 MHz modulation is still present in both Q-tipped and tapered cells. The characteristic length for the larger frequency modulation is approximately 5 cm, which is estimated using f= c/2nL where c is the speed of light in the vacuum, n is the fused silica group index at 1550 nm . Since the aforementioned characteristic length is close to the length of the Q-tipped PBGF in the PMC, this modulation may arise due to the back reflection of the light from the Q-tipped end and the PBGF to SMF splice end. In contrast, the characteristic length of the modulation with small frequency is approximately 4 m and maybe due to measurement artifacts.

The etalon-like effect on the wing also masks the $H^{12}C^{13}CH$ line close to the P13 line. $H^{12}C^{13}CH$ has a peak approximately 1500 MHz away from P13 line center, which can be used as a frequency calibration check. As shown in Fig. 6.7, the $H^{12}C^{13}CH$ line is masked by an etalon-like effect.

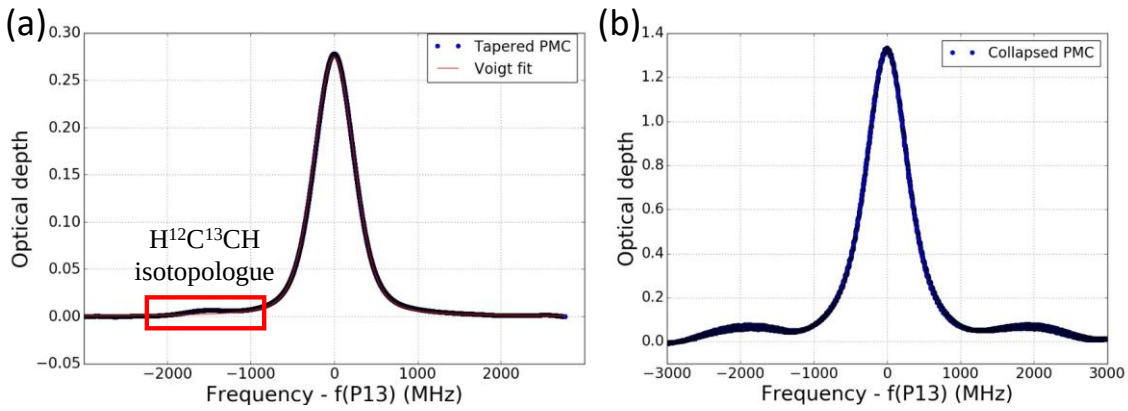

Fig. 6.7. (a) Measured optical depth fit to Voigt profile for tapered PMC no. 52 (length = 6.0 cm, Pa = 3.1 torr, Pc = 23.0 torr) with reduced etalon-like effect on the line wings of the optical depth. (b) Collapsed PMC no. 40 (length = 8.0 cm, Pa = 16.2 torr, Pc = 31.6 torr) with etalon-like effect on the line wings.

Long-term stability of the cells

One important question for sealed fiber cells is how stable are they in terms of partial pressures over time. We address this question by remeasuring the partial pressures for both connectorized and unconnectorized cells made with two different techniques of tapering and Q-

tipping that had been previously measured. While the measurements for cell no. 53 are approximately 6 months and for PMCs no. 17 and 19 one year apart, the results show no change within the error bars on Table 6.4. These errors are associated with the extracted voltage offset for absorption voltage shown in Fig. 6.3(a) which causes error for finding the partial pressures. The discrepancy implies that there are measurement artifacts, but the observed small pressure change is not likely to be due to outgassing or leaking. The key results are tabulated in Table 6.4.

In addition, line center shift does not change because as Table 6.4 shows, partial pressures remain constant within error bars.

Table 6.4 Long-term stability of connectorized tapered PMC no. 53 and unconnectorized Q-tipped PMCs no. 17 and 19.

PMC no.	Data date	Voigt FWHM (MHz)	P_a (torr)	P_c (torr)
Tapered connectorized cell no. 53	1-25-2018	569 ± 24	2.9 ± 0.5	11.4 ± 2.7
	7-12-2018	551 ± 5	3.0 ± 0.2	15.1 ± 3.1
Q-tipped unconnectorized cell no.19	1-30-2017	606 ± 16	9.6 ± 0.8	21.4 ± 2.6
	6-4-2018	588 ± 22	12.7 ± 2.9	14.1 ± 5.9
Q-tipped unconnectorized cell no.17	1-30-2017	705 ± 47	18.1 ± 3.5	27.3 ± 4.6
	6-4-2018	706 ± 43	19.1 ± 3.5	25.8 ± 3.9

Chapter 7 - Conclusion

Short acetylene-filled PMCs (6-10 cm) were fabricated in the pressure-broadened regime, in the form of a connectorized all-fiber device that can be mounted into photodetectors for moderate accuracy frequency measurements and may be connected to 400 μm core MMF. This PMC can fit into laser devices as an optical reference. In this work, the butt coupling transmission increased to 61% into a 400 μm core MMF and 52% into a 200 μm core MMF, and the 13% etalon-like effect that appeared on the wings of the optical depth in the Q-tipping method was reduced to less than 1% by using the tapering method. We were able to find the line center shift of the tapered connectorized PMC no. 53 with accuracy of 10 MHz, which is comparable to NIST SRM 2517a accuracy on the P13 absorption line center. Moreover, experimental data of the frequency between a sub-Doppler reference and the connectorized tapered PMC no. 53 center shows 15.4 ± 3.3 MHz separation. Although some PMCs are contaminated between 50-86%, contaminant pressure only causes a small shift of less than 15.4 MHz on the PMC center with respect to the sub-Doppler feature, and the PMCs are still useful devices for moderate accuracy frequency measurements. Finally, results of the long-term stability show no changes in total pressure within uncertainties over a period of at least 5 months for the PMCs.

Appendix A - Safety procedure for epoxy

Part of the connectorization process consists of injecting the epoxy (long pot life, room temperature cure epoxy from THORLABS, part number: F112) in the FC/PC connector and then pushing the PMC and wait for the epoxy to be cured. Since the aforementioned epoxy is poisonous and causes serious skin and eye irritation, careful actions need to be done during the process of epoxying the PMC.

Setup

Set up the following materials in the LUMOS lab on a work surface near the vent as shown in the Figures.

a) Chemical resistant liquid proof gloves

b) Mask

c) Safety Glasses

d) FC/PC fiber connector and fiber to be connected

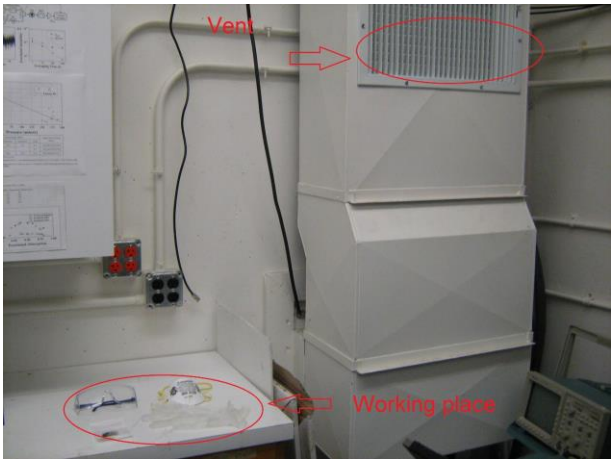

Set up the following materials inside the fume hood located outside the LUMOS lab.

a) Syringe and its cap

b) Epoxy

c) Scissors

d) White jar

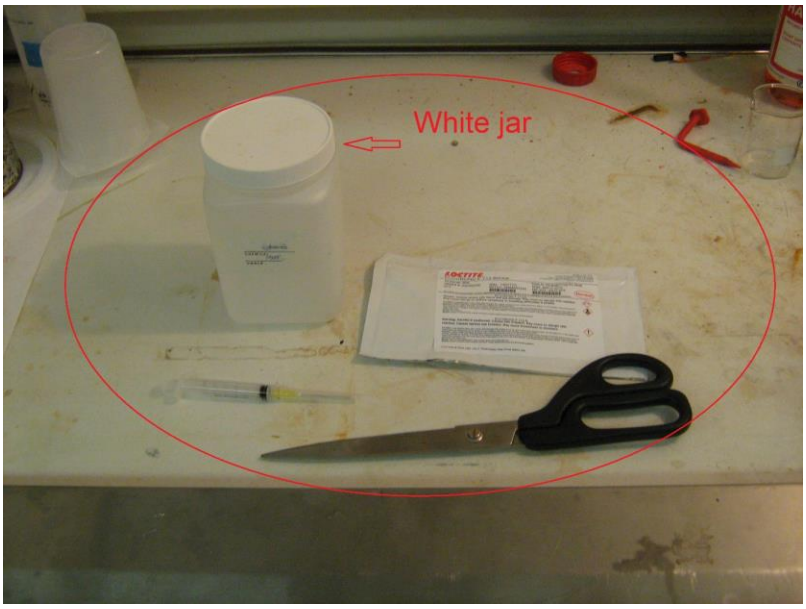

In addition, the following materials outside, next to the hood.

a) Chemical resistant liquid proof Gloves

b) Safety glasses

c) Ziploc bag

d) Mask

e) Chemical label

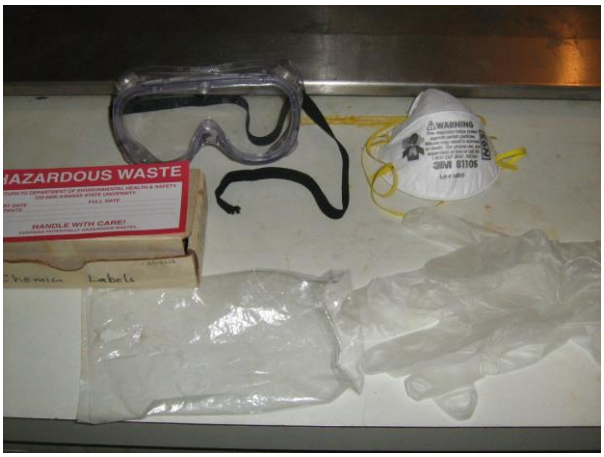

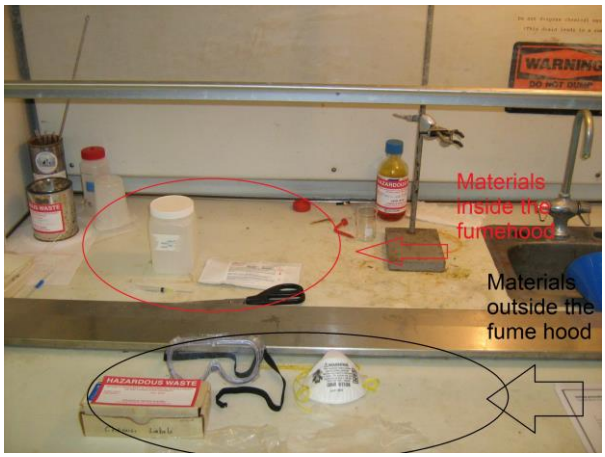

The following figure shows the storage cabinet where the epoxies are stored. This cabinet is located outside the LUMOS lab and close to the fume hood.

Fume Hood Procedures

1. Label the white jar with hazardous waste with the date and the user's name.
2. Turn on the hood.
3. Wear gloves, glasses, and the mask.

4. Mix the epoxy inside the hood.
5. Cut the corner of the epoxy with scissors.
6. Fill the syringe with epoxy and put the cap on it.
7. Put the syringe in the Ziploc bag and seal.
8. Put the remnants of the epoxy (epoxy bag) in the white jar.
9. Wipe off the scissors and place the wipe in the jar.
10. Place your gloves in the white jar.
11. Place the glasses and the mask where they belong.
12. Take the syringe sealed in bag to the LUMOS lab.

LUMOS Lab Procedures

1. Open the vent in the LUMOS lab.
2. Wear gloves, glasses, and mask.
3. Open Ziploc bag, remove syringe cap, and prepare fiber inside connector.
4. Inject epoxy into connector.
5. Leave the connector next to the vent while the process of curing is done. When you are done with the syringe, put the cap on the syringe.
6. Place the Syringe in the Ziploc bag again.
7. Place the gloves in Ziploc bag and seal it.
8. Place the glasses and the mask where they belong.
9. Leave a warning note with your name and date next to the connector that nobody should touch the connector.

10. Place the Ziploc bag into the white jar in the hood.
11. Post a sign on the fume's glass that tells people not to turn the hood off and to contact you if there are questions.
12. Wash your hands thoroughly with soap and water.

    Leave the white jar inside the fume hood, with cap off for 24 hrs. After 24 hours, secure cap on white jar, turn off the fume hood, and get rid of the note on the glass.
13. Place the white jar with the cap on in chemical cabinet -where the epoxy is stored- after the 24-hour hardening period.
14. When the white jar is full, take it upstairs, leave it in room CW 4, and call EH&S to take care of the jar. (phone number:532-5856)

Caution:

The epoxy is made of two different chemical substances. Whenever one of them touches your skin, do the following.

ECCOBOND F112-H

Response: If on skin (or hair): Remove all contaminated clothing immediately. Wash contaminated clothing before reuse.

ECCOBOND F112-R

Response: if on skin: wash with plenty of soap and water.

Appendix B - Python code to convert ring cavity data to relative frequency

```
"""
Created on Mon May 22 14:38:15 2017
Python version 2.7
@authors: Brian Washburn, Sajed Hosseini-Zavareh, and Ryan Luder
Final version

Script to convert ring cavity data to a relative frequency in MHz
The program takes the ring cavity data and finds the peaks and respective
indices.
Next, the program converts the peaks to frequency using the cavity FSR.
This is the
fit to a third order polynomial and a calibrated relativte frequency axis
is created

The program uses PEAKDET to find peaks and CALIBRATE_FREQ to calibrate

Besides the data, the user must input
The user must input in the code below
        f1: starting index of data to calibrate
        f2: stopping index of data to calibrate
        ramp_slope: slope of ramp
        peak_delta : the peak height to search for using peakdet

"""

import sys
import numpy as np
from matplotlib import pyplot as plt
from numpy import NaN, Inf, arange, isscalar, asarray, array, linspace

#-----------------------------------------------------------------------
```

```
def peakdet(v, delta, x = None):
    """
    Converted from MATLAB script at http://billauer.co.il/peakdet.html

    Returns two arrays

    function [maxtab, mintab]=peakdet(v, delta, x)
    %PEAKDET Detect peaks in a vector
    %        [MAXTAB, MINTAB] = PEAKDET(V, DELTA) finds the local
    %        maxima and minima ("peaks") in the vector V.
    %        MAXTAB and MINTAB consists of two columns. Column 1
    %        contains indices in V, and column 2 the found values.
    %
    %        With [MAXTAB, MINTAB] = PEAKDET(V, DELTA, X) the indices
    %        in MAXTAB and MINTAB are replaced with the corresponding
    %        X-values.
    %
    %        A point is considered a maximum peak if it has the maximal
    %        value, and was preceded (to the left) by a value lower by
    %        DELTA.

    % Eli Billauer, 3.4.05 (Explicitly not copyrighted).
    % This function is released to the public domain; Any use is allowed.

    """
    maxtab = []
    mintab = []

    if x is None:
        x = arange(len(v))

    v = asarray(v)

    if len(v) != len(x):
        sys.exit('Input vectors v and x must have same length')
```

```
    if not isscalar(delta):
        sys.exit('Input argument delta must be a scalar')

    if delta <= 0:
        sys.exit('Input argument delta must be positive')

    mn, mx = Inf, -Inf
    mnpos, mxpos = NaN, NaN

    lookformax = True

    for i in arange(len(v)):
        this = v[i]
        if this > mx:
            mx = this
            mxpos = x[i]
        if this < mn:
            mn = this
            mnpos = x[i]

        if lookformax:
            if this < mx-delta:
                maxtab.append((mxpos, mx))
                mn = this
                mnpos = x[i]
                lookformax = False
        else:
            if this > mn+delta:
                mintab.append((mnpos, mn))
                mx = this
                mxpos = x[i]
                lookformax = True

    return array(maxtab), array(mintab)

#---------------------------------------------------------------------
```

```
def calibrate_freq(ringdata,f1,f2,ramp_slope,peakdelta):
    """
    Calibrates frequency axis from ring cavity data
    Inputs
        ringdata : ring cavity data
        f1 : starting index of data to calibrate
        f2 : stopping index of data to calibrate
        ramp_slope: slope of ramp
        peak_delta : the peak height to search for using peakdet

    Output
        cal_freq : the calibrated frequency in MHz for a given ring cavity
FSR
    """
    ring_cut=ringdata[f1:f2]    # truncate the data to peak search
    indices=np.linspace(0,f2-f1-1,f2-f1) # create index array

    # create peaks from ring cut
    ring_cut = np.abs(ring_cut-max(ring_cut))

    # find the peaks
    maxtab, mintab = peakdet(ring_cut, peakdelta, x=indices) # get peaks
    peakpos=array(maxtab)[:,0]        # peak positions on x axis
    pp=array(maxtab)[:,1]           # peak values on y axis

    plt.figure(3)
    plt.plot(indices,ring_cut)
    plt.plot(peakpos,pp,'ro',label='found peaks')
    plt.grid(True)
    plt.legend(bbox_to_anchor=(1.05, 1), loc=0, borderaxespad=0.)

#    fsr = 90.7  # ring cavity free spectral range in MHz
    fsr = 180.00

    # Creates a frequency array based on the peaks, and the direction of
the ramp.
```

```
    if ramp_slope=='+':
        freq=linspace(0,-fsr*(len(peakpos)-1),len(peakpos))
        freq=freq-min(freq)
    if ramp_slope=='-':
        freq=linspace(0,fsr*(len(peakpos)-1),len(peakpos))#adding the freq
array to peakpos

    # fitting freq vs peak indices to a 3rd order polynomial
    coeffs=np.polyfit(peakpos, freq, 3)
    p3=np.poly1d(coeffs)
    cal_freq = p3(indices) # create calibrated frequency axis

    # plot freq vs peakpos data
    plt.figure(4)
    plt.plot(peakpos,freq,'bo',)
    plt.plot(peakpos,p3(peakpos),'r')
    plt.xlabel('points')
    plt.ylabel('relative transmission')
    plt.title('Frequency fitting')
    plt.grid(True)
    plt.show()

    return cal_freq
#-------------------------------------------------------------------------

#   Load the Data
#filename='RPDAQ_31-05-17_122540.txt'
#directory ='C:\\Users\\Brian\\Work\\Data\\HOFGLAS abs data\\060117\\'

filename='RPDAQ_26-06-17_100803.txt'
directory ='C:\Users\Brian\Work\Data\PMC abs data for paper\\'
pathname=  directory + filename

#   Set each variable: (time,Ramp,cell,ring,ref) equal to a column of the
data
```

```
#time, cell, ring, ref, ramp = np.loadtxt(pathname, delimiter=',',
usecols=(0,1,2,3,4), unpack=True)
c0, c1, c2, c3, c4 = np.loadtxt(pathname, delimiter=',',
usecols=(0,1,2,3,4), unpack=True)


#plot all 4 inputs Versus index.
plt.figure(1)
plt.plot(c1)
plt.show()

plt.figure(2)
plt.plot(c2)
plt.show()

plt.figure(3)
plt.plot(c3)
plt.show()

pt = raw_input("Calibrate frequency data? [y/n]: ")
if pt =='n':  sys.exit() # quit if you dont want to calibrate

#Choose the bounds (f1,f2) of the data to fit, the derivative of the ramp
(+/-),
#the distance between ring cavity peaks, and the minimum amplitude of ring
cavity peaks.
f1=4000                 # beginning index
f2=12000                # ending index
ramp_slope='+'          # ramp slope
peak_delta=.010          # peak height to search for

# generated cut data
c0c=c0[f1:f2]
c1c=c1[f1:f2]       # cell transmission array, adding back in a voltage
offset
c2c=c2[f1:f2]      # Ramp array
```

```
c3c=c3[f1:f2]      #reference transmission array, adding back in a voltage
offset
c4c=c4[f1:f2]        #ring cavity array

# callibrate data using calibrate function
ring = c3
cal_freq = calibrate_freq(ring,f1,f2,ramp_slope,peak_delta)

# write fit data to a text file
pt = raw_input("Save data? [y/n]: ")
if pt =='y':
    savefile=filename[0:len(filename)-4]+'_calibrated_frequency.txt'     #
file name
    pathname=  directory + savefile # path name
    head='time\t cell\t ramp\t hof\t ring\t calfreq' # file header
    np.savetxt(pathname,np.vstack((c0c, c1c, c2c, c3c, c4c, cal_freq)).T,\
    fmt=['%.7e','%.7e','%.7e','%.7e','%.7e','%.7e'],       delimiter='\t',
header=head, comments='')
```

Appendix C - Python code to fit P13 line to Voigt profile

```
"""
Created on 4/2017
Python version 2.7
@author: Brian Washburn, Sajed Hosseini-Zavareh, and Ryan Luder
Version 4 of voigt_fit_P13_absorption.py

Script to fit P13 data to a Voigt profile and finding the partial
pressures

lmfit from http://lmfit.github.io/lmfit-py/intro.html

To install lmfit you must download and install it (not found in Anaconda)
1) In Windows open the Command Prompt (Start Menu>Programs>Accesories)
2) In the command prompt type 'pip install lmfit'

References
[1] Olivero, J. J.; R. L. Longbothum (February 1977).
"Empirical fits to the Voigt line width: A brief review".
Journal of Quantitative Spectroscopy and Radiative Transfer. 17 (2): 233-
236.
[2] NIST data https://www-s.nist.gov/srmors/view_datafiles.cfm?srm=2517A
[3] Swann and Gilbert JOSAB

"""
from scipy import integrate
import numpy as np
from matplotlib import pyplot as plt
from lmfit.models import VoigtModel, LinearModel
import os
from lmfit import  Model
import matplotlib.gridspec as gridspec
# universal constants
kb = 1.3806503*1e-23  # J/K, Boltzmann constant
amu=1.66054e-27       # atomic mass unit in kg
```

```
c = 2.99792458*1e8    # m/s, speed of light
c_nmTHz=2.99792458*(10**9)*(10**-4) # speed of light in nm*THz

# HITRAN database spectral line strength
S = 1.035e-20 # in units of cm-1/(molecules 1/cm2) taken from HITRAN
database
S = S/100**2  # convert to cm-1/(molecules 1/m2)
S = S*(c*100) # convert to Hz/(molecules 1/m2) using 1 cm-1 is equal to
29.97 GHz

#------------------------------------------------------------------------
def compute_fwhm(x,y):
# compute the fwhm of a function y(x)
    ymax=max(y)       # peak absorption at line center
    y=y/ymax
    index1 = 0
    index2 = 0
    for i in range(len(y)):
        if y[i] >= 0.5 and index1 == 0:
            if abs(y[i] - 0.5) > abs(y[i-1] - 0.5):
                index1 = i -1
            else:
                 index1 = i
        elif y[i] <= 0.5 and index1 > 0:
            if abs(y[i] - 0.5) > abs(y[i-1] - 0.5):
                index2 = i - 1
            else:
                index2 = i
            break
    bx1 = x[index1]
    bx2 = x[index2]
    return abs(bx1-bx2)

def voigt_fwhm(gfwhm,lfwhm):
# use approximate express to relate voigt fwhm to gaussian and lorenzian
fwhm
```

```
# expression from [1]
    return 0.5346*lfwhm + np.sqrt(0.2166*lfwhm**2 + gfwhm**2)

def sigmaG(T,m,f0):
# Gaussian width sigma as a function of temperature (in Kelvin)
# gaussian fwhm is equal to 2*Sqrt(2*ln(2))*sigma = 2.355 Sigma
     return f0*np.sqrt(kb*T/(m*c**2)) # error here fixed on 4/2017

def gL(p):
# Compute lorenztian gamma from fitting NIST SRM2517 data widths
    b=11.467e6  # slope of 11.4 MHz per torr, from Ref [3], Table 4
    a=58.465e6  # intercept
    return (b*p+a)/2

def find_nearest(arr,v):
# find index of elements in arr to nearest value v
    idx = (np.abs(arr - v)).argmin()
    return idx

def df_to_dl(df,f0):
# convert df in Hz to dl in meters
    return (c/f0**2)*df

#-------------------------------------------------------------------------
plt.close('all')

# system parameters
l0=1532.83042e-9        # P13 center wavelength in m from [4]
f0=c/l0                 # center frequency in Hz
f0THz = f0/1e12         # center frequency in THz
m=26*amu                # mass in kg of acetylene molecule
T=298.0                 # temperature in Kelvin
L = 0.06              # PMC length

#   Load the Data taken by Sajed
```

```
filename='RPDAQ_25-01-18_104822_calibrated_frequency FSR=93_filterred cell
noise .txt'
directory  ='R:\\LUMOS  (Corwin)\\Researchers\\sajed\\cell  #53  set-up
pressure 11.98 torr 78% transmission 6 cm\\'
pathname=  directory + filename
c0, c1, c2, c3, c4, c5 = np.loadtxt(pathname, skiprows=1, delimiter='\t',
usecols=(0,1,2,3,4,5), unpack=True)
# c2 pmc
# c5 frequency

print
'_____________________________________________________________________________'
print 'Running %s ...  ' % os.path.basename(__file__)
print ' '
print 'Fit P13 acetylene line'
print'\t file : %s' % filename



argc1min = np.argmin(c1)
c5 = c5 - c5[argc1min]

#plt.figure(1)
#plt.plot(c5,c2)

## create absolute frequency axis based on frequency of P13 line
pmcT = c1/c1[0]
fpmc = c5*1e6 + f0  # convert to relative frequency to absolute frequency

plt.figure(1)
plt.plot((fpmc-f0)/1e6 ,pmcT,'r',label="data")
plt.ylabel('transmission')
plt.xlabel('frequency - f(P13) (MHz)')
plt.grid(True)

# create x and y arrays for fitting
x = fpmc/1e12  # do fitting in units of THz
```

```
y = pmcT

# compute relative absorption
#    Using Beer's Law I(f)=Io exp(-a(f)*L), so a(f)*L=-ln(I(f)/Io), Let
y=a*L
y=-np.log(y)



# compute sigma (in THz) for fit
sig=sigmaG(T,m,f0)/1e12      # gaussian width at given temperature

# fit data



mod = VoigtModel()
pars = mod.guess(y, x=x)
pars['sigma'].set(value=sig, vary=False, expr='') # Fit sigma to 440MHz
    # due to room temp
#pars['a'].set(value=0,vary=True,expr='')
#pars['omega'].set(value=0,vary=True,expr='')
#pars['theta'].set(value=0,vary=True,expr='')
pars['gamma'].set(value=70e-6, vary=True, expr='') # set inital gamma
pars['amplitude'].set(value=0.0018, vary=True, expr='')
out  = mod.fit(y, pars, x=x)
rpt=out.fit_report(min_correl=0.25)
print(rpt)



# print and plot results
print(out.fit_report())
# plot residuals
plt.figure(13)
out.plot_residuals()
```

```
vv=out.residual
plt.grid(True)

# get fitting parameters
bfp=out.params              # ordered dictionary of parameters
fcen=bfp['center'].value    # get center value
fcener=bfp['center'].stderr # get center value error
famp=bfp['amplitude'].value    # get center value
print 'Fit P13 acetylene line'
print 'Center frequency from fit is ', fcen, '+/-', fcener , 'THz.'
print 'Amplitude from fit is ', famp, '.'

sigma = bfp['sigma'].value
gamma = bfp['gamma'].value

# compute lorenzian and gaussian fwhm
lfwhm = 2*gamma  # lorenzian fwhm
gfwhm = sigma*2*np.sqrt(2*np.log(2)) # gaussian fwhm
print 'Gaussian sigma = %0.3f MHz' %(sigma*1e6)
print 'Gaussian FWHM = %0.3f MHz' %(gfwhm*1e6)
print 'Lorenztian gamma = %0.3f MHz' %(gamma*1e6)
print 'Lorenztian FWHM = %0.3f MHz' %(lfwhm*1e6)

# compute voigt fwhm
vfwhmfit=compute_fwhm(x,out.best_fit)  #compute fwhm from fit
vcfwhm  =  voigt_fwhm(gfwhm,lfwhm)  #  compute  fwhm  from  approximate
expression
print 'Voigt fwhm is %0.3f MHz from fit, %0.3f MHz from approximation'
%(vfwhmfit*1e6,vcfwhm*1e6)

# compute pressure from Area
A=np.abs(np.trapz(y,x=x))
A= A*1e12  # area has units of THz/molecule, convert to Hz/molecule
pfit =(A*kb*T/(L*S))/133.32 # pressure in torr, 1 torr = 133.32 pascal
print ' '
print 'The pressure from Area  is %0.3f torr' % pfit
```

```
# compute pressure from lorenztian gamma fitting  lfwhm = b*p + a
b=11.36e6  # slope of 11.4 MHz per torr, from Ref [3], Table 4

pfit2 = ((lfwhm*1e12)/b)
print 'The pressure from the fitting gamma and igmoring NIST relation is
%0.3f torr' % pfit2
# solve for air partial pressure

Lorenztian_gamma=gamma*1e6  # Lorenztian gamma from the fitting
air_broadening_factor=3.067 # air_broadening_factor for P13 (From HITRAN
data base)
b=b/1e6
Pair1= (Lorenztian_gamma-((b/2)*pfit))/air_broadening_factor

print 'Air partial  pressure  is %0.3f torr' % Pair1
cont= Pair1/(Pair1+pfit) *100
print'contamination percentage %0.3f ' % cont
# plot data and fit
plt.figure(2)
plt.plot((x-f0THz)*1e6, y, 'bx', label="experimental Data")
plt.ylabel('Optical depth',fontsize=25)
plt.xlabel('frequency - f(P13) (MHz)',fontsize=23)
plt.legend(bbox_to_anchor=(1, 1), loc=0, borderaxespad=0.)
plt.tick_params(axis='both',which='major',labelsize=18)
#plt.xlim(-2000,2000)
#plt.ylim(0,2)
plt.grid(True)

plt.figure(2)
plt.plot((x-f0THz)*1e6,out.best_fit,'r',label="Fit")
plt.ylabel('Optical depth',fontsize=25)
plt.xlabel('Relative frequency (MHz)',fontsize=23)
plt.legend(bbox_to_anchor=(1, 1), loc=0, borderaxespad=0.)
plt.tick_params(axis='both',which='major',labelsize=18)
plt.legend(bbox_to_anchor=(1, 1), loc=0, borderaxespad=0.)
```

```
#plt.ylim(0,2)
plt.xlim(-2000,2000)
plt.grid(True)

plt.figure(4)
plt.plot((x-f0THz)*1e6, y-out.best_fit, 'b')
plt.ylabel('data-fit')
plt.xlabel('Relative frequency')
plt.title('Difference between Raw Data and Fit')
plt.ylim(-0.05,0.05)
#plt.xlim(-2000,2000)
plt.grid(True)
```

Appendix D - Permissions

Permission for Fig. 1.2

SPRINGER NATURE LICENSE TERMS AND CONDITIONS

Dec 03, 2018

This Agreement between Mr. Sajed Hosseini ("You") and Springer Nature ("Springer Nature") consists of your license details and the terms and conditions provided by Springer Nature and Copyright Clearance Center.

License Number	4481561457224
License date	Dec 03, 2018
Licensed Content Publisher	Springer Nature
Licensed Content Publication	Applied Physics B: Lasers and Optics
Licensed Content Title	Portable optical frequency standard based on sealed gas-filled hollow-core fiber using a novel encapsulation technique
Licensed Content Author	Marco Triches, Anders Brusch, Jan Hald
Licensed Content Date	Jan 1, 2015
Licensed Content Volume	121
Licensed Content Issue	3
Type of Use	Thesis/Dissertation
Requestor type	academic/university or research institute
Format	print and electronic
Portion	figures/tables/illustrations
Number of figures/tables /illustrations	1
Will you be translating?	no
Circulation/distribution	<501
Author of this Springer Nature content	no
Title	ACETYLENE-FILLED PRESSURE BROADENED SHORT PHOTONIC MICROCELLS
Institution name	Kansas state university
Expected presentation date	Dec 2018
Order reference number	17
Portions	Figure 1
Requestor Location	Mr. Sajed Hosseini-Zavareh 1700 Hillcrest Dr. Apt. P#4 MANHATTAN, KS 66502 United States Attn: Mr. Sajed Hosseini-Zavareh
Billing Type	Invoice
Billing Address	Mr. Sajed Hosseini-Zavareh 1700 Hillcrest Dr. Apt. P#4

MANHATTAN, KS 66502
United States
Attn: Mr. Sajed Hosseini-Zavareh

Total 0.00 USD

Terms and Conditions

Springer Nature Terms and Conditions for RightsLink Permissions

Springer Nature Customer Service Centre GmbH (the Licensor) hereby grants you a non-exclusive, world-wide licence to reproduce the material and for the purpose and requirements specified in the attached copy of your order form, and for no other use, subject to the conditions below:

1. The Licensor warrants that it has, to the best of its knowledge, the rights to license reuse of this material. However, you should ensure that the material you are requesting is original to the Licensor and does not carry the copyright of another entity (as credited in the published version).

   If the credit line on any part of the material you have requested indicates that it was reprinted or adapted with permission from another source, then you should also seek permission from that source to reuse the material.

2. Where **print only** permission has been granted for a fee, separate permission must be obtained for any additional electronic re-use.

3. Permission granted **free of charge** for material in print is also usually granted for any electronic version of that work, provided that the material is incidental to your work as a whole and that the electronic version is essentially equivalent to, or substitutes for, the print version.

4. A licence for 'post on a website' is valid for 12 months from the licence date. This licence does not cover use of full text articles on websites.

5. Where **'reuse in a dissertation/thesis'** has been selected the following terms apply: Print rights of the final author's accepted manuscript (for clarity, NOT the published version) for up to 100 copies, electronic rights for use only on a personal website or institutional repository as defined by the Sherpa guideline (www.sherpa.ac.uk/romeo/).

6. Permission granted for books and journals is granted for the lifetime of the first edition and does not apply to second and subsequent editions (except where the first edition permission was granted free of charge or for signatories to the STM Permissions Guidelines http://www.stm-assoc.org/copyright-legal-affairs/permissions/permissions-guidelines/), and does not apply for editions in other languages unless additional translation rights have been granted separately in the licence.

7. Rights for additional components such as custom editions and derivatives require additional permission and may be subject to an additional fee. Please apply to Journalpermissions@springernature.com/bookpermissions@springernature.com for these rights.

8. The Licensor's permission must be acknowledged next to the licensed material in print. In electronic form, this acknowledgement must be visible at the same time as the figures/tables/illustrations or abstract, and must be hyperlinked to the journal/book's homepage. Our required acknowledgement format is in the Appendix below.

9. Use of the material for incidental promotional use, minor editing privileges (this does not include cropping, adapting, omitting material or any other changes that affect the meaning, intention or moral rights of the author) and copies for the disabled are permitted under this licence.

10. Minor adaptations of single figures (changes of format, colour and style) do not require the Licensor's approval. However, the adaptation should be credited as shown in Appendix

below.

Appendix — Acknowledgements:

For Journal Content:
Reprinted by permission from **[the Licensor]**: **[Journal Publisher** (e.g. Nature/Springer/Palgrave)] **[JOURNAL NAME] [REFERENCE CITATION** (Article name, Author(s) Name), **[COPYRIGHT]** (year of publication)

For **Advance Online Publication papers:**
Reprinted by permission from **[the Licensor]**: **[Journal Publisher** (e.g. Nature/Springer/Palgrave)] **[JOURNAL NAME] [REFERENCE CITATION** (Article name, Author(s) Name), **[COPYRIGHT]** (year of publication), advance online publication, day month year (doi: 10.1038/sj.[JOURNAL ACRONYM].)

For Adaptations/Translations:
Adapted/Translated by permission from **[the Licensor]**: **[Journal Publisher** (e.g. Nature/Springer/Palgrave)] **[JOURNAL NAME] [REFERENCE CITATION** (Article name, Author(s) Name), **[COPYRIGHT]** (year of publication)

Note: For any republication from the British Journal of Cancer, the following credit line style applies:

Reprinted/adapted/translated by permission from **[the Licensor]**: on behalf of Cancer Research UK: : **[Journal Publisher** (e.g. Nature/Springer/Palgrave)] **[JOURNAL NAME] [REFERENCE CITATION** (Article name, Author(s) Name), **[COPYRIGHT]** (year of publication)

For **Advance Online Publication** papers:
Reprinted by permission from The **[the Licensor]**: on behalf of Cancer Research UK: **[Journal Publisher** (e.g. Nature/Springer/Palgrave)] **[JOURNAL NAME] [REFERENCE CITATION** (Article name, Author(s) Name), **[COPYRIGHT]** (year of publication), advance online publication, day month year (doi: 10.1038/sj.[JOURNAL ACRONYM])

For Book content:
Reprinted/adapted by permission from **[the Licensor]**: **[Book Publisher** (e.g. Palgrave Macmillan, Springer etc) **[Book Title]** by **[Book author**(s)] **[COPYRIGHT]** (year of publication)

Other Conditions:

Version 1.1

Permission for Fig. 1.3

PU pubscopyright <copyright@osa.org>
To: Hosseini-Zavareh, Sajed; pubscopyright <copyright@osa.org>;

Thu 11/29/2018 2:49 PM

Dear Sajed Hosseini,

Thank you for contacting The Optical Society.

For the use of figure 1 from P. S. Light, F. Couny, and F. Benabid, "Low optical insertion-loss and vacuum-pressure all-fiber acetylene cell based on hollow-core photonic crystal fiber," Opt. Lett. 31, 2538-2540 (2006):

OSA considers your requested use of its copyrighted material to be Fair Use under United States Copyright Law. It is requested that a complete citation of the original material be included in any publication.

While your publisher should be able to provide additional guidance, OSA prefers the below citation formats:

For citations in figure captions:

[Reprinted/Adapted] with permission from ref [x], [Publisher]. (with full citation in reference list)

For images without captions:

Journal Vol. #, first page (year published) An example: Opt. Lett. 31, 2538 (2006)

Please let me know if you have any questions.

Kind Regards,

Rebecca Robinson

Rebecca Robinson
November 29, 2018
Authorized Agent, The Optical Society

The Optical Society (OSA)
2010 Massachusetts Ave., NW
Washington, DC 20036 USA
www.osa.org

Reflecting a Century of Innovation

Permission for Fig. 4.3

Copyright Clearance Center RightsLink®

Home | Account Info | Help

Taylor & Francis
Taylor & Francis Group

Title: Linear and nonlinear optical properties of hollow core photonic crystal fiber
Author: F. Benabid, P.J. Roberts
Publication: Journal of Modern Optics
Publisher: Taylor & Francis
Date: Jan 20, 2011
Rights managed by Taylor & Francis

Logged in as:
Sajed Hosseini-Zavareh
Account #:
3001375677
LOGOUT

Thesis/Dissertation Reuse Request

Taylor & Francis is pleased to offer reuses of its content for a thesis or dissertation free of charge contingent on resubmission of permission request if work is published.

BACK | CLOSE WINDOW

References

1. W. Demtroder, *Laser Spectroscopy Basic Concepts and Instrumentation*, Third ed. (Springer,1996).
2. R. Thapa, "Doppler-free spectroscopy of acetylene in near infrared spectral region inside photonic band gap fiber," Master's thesis, Kansas State University (2005).
3. K. Knabe, "Using saturated absorption spectroscopy on acetylene-filled hollow-core fibers for absolute frequency measurements," PhD thesis, Kansas State University (2010).
4. C. Wang, "Optical frequency references in acetylene-filled hollow-core optical fiber and photonic microcells," PhD thesis, Kansas State University (2015).
5. B. R. Washburn, "Dispersion and nonlinearities associated with supercontinuum generation in microstructure fibers," PhD thesis, Georgia Institute of Technology (2002).
6. M. Herman, A. Campargue, M. I. E. Idrissi, and J. V. Auwera, "Vibrational Spectroscopic Database on Acetylene, ($^{12}C_2H_2$, $^{12}C_2D_2$, and $^{13}C^2H^2$)," Journal of Physical and Chemical Reference Data **32**, 921-1361 (2003).
7. W. C. Swann and S. L. Gilbert, "Pressure-induced shift and broadening of 1510–1540-nm acetylene wavelength calibration lines," J. Opt. Soc. Am. B **17**, 1263-1270 (2000).
8. R. F. Cregan, B. J. Mangan, J. C. Knight, T. A. Birks, P. S. J. Russell, P. J. Roberts, and D. C. Allan, "Single-Mode Photonic Band Gap Guidance of Light in Air," Science **285**, 1537-1539 (1999).
9. C. M. Smith, N. Venkataraman, M. T. Gallagher, D. Müller, J. A. West, N. F. Borrelli, D. C. Allan, and K. W. Koch, "Low-loss hollow-core silica/air photonic bandgap fibre," Nature **424**, 657 (2003).
10. F. Benabid, J. C. Knight, G. Antonopoulos, and P. S. J. Russell, "Stimulated Raman Scattering in Hydrogen-Filled Hollow-Core Photonic Crystal Fiber," Science **298**, 399-402 (2002).
11. F. Benabid, G. Bouwmans, J. C. Knight, P. S. Russell, and F. Couny, "Ultrahigh efficiency laser wavelength conversion in a gas-filled hollow core photonic crystal fiber by pure stimulated rotational Raman scattering in molecular hydrogen," Physical review letters **93**, 123903 (2004).
12. D. G. Ouzounov, F. R. Ahmad, D. Müller, N. Venkataraman, M. T. Gallagher, M. G. Thomas, J. Silcox, K. W. Koch, and A. L. Gaeta, "Generation of Megawatt Optical Solitons in Hollow-Core Photonic Band-Gap Fibers," Science **301**, 1702-1704 (2003).
13. T. Ritari, J. Tuominen, H. Ludvigsen, J. C. Petersen, T. Sørensen, T. P. Hansen, and H. R. Simonsen, "Gas sensing using air-guiding photonic bandgap fibers," Opt. Express **12**, 4080-4087 (2004).
14. F. Benabid, P. S. Light, F. Couny, and P. S. J. Russell, "Electromagnetically-induced transparency grid in acetylene-filled hollow-core PCF," Opt. Express **13**, 5694-5703 (2005).
15. S. Ghosh, J. E. Sharping, D. G. Ouzounov, and A. L. Gaeta, "Resonant optical interactions with molecules confined in photonic band-gap fibers," Physical review letters **94**, 093902 (2005).
16. F. Benabid, F. Couny, J. C. Knight, T. A. Birks, and P. S. J. Russell, "Compact, stable and efficient all-fibre gas cells using hollow-core photonic crystal fibres," Nature **434**, 488 (2005).

17. M. Triches, A. Brusch, and J. Hald, "Portable optical frequency standard based on sealed gas-filled hollow-core fiber using a novel encapsulation technique," Applied Physics B **121**, 251-258 (2015).
18. P. S. Light, F. Couny, and F. Benabid, "Low optical insertion-loss and vacuum-pressure all-fiber acetylene cell based on hollow-core photonic crystal fiber," Opt. Lett. **31**, 2538-2540 (2006).
19. C. Wang, N. V. Wheeler, C. Fourcade-Dutin, M. Grogan, T. D. Bradley, B. R. Washburn, F. Benabid, and K. L. Corwin, "Acetylene frequency references in gas-filled hollow optical fiber and photonic microcells," Appl. Opt. **52**, 5430-5439 (2013).
20. R. Luder, S. Hosseini-Zavareh, C. Wang, M. Thirugnanasambandam, B. Washburn, and K. Corwin, "Short Acetylene-Filled Photonic Bandgap Fiber Cells Toward Practical Industry Standards," in *Conference on Lasers and Electro-Optics*, OSA Technical Digest (2016) (Optical Society of America, 2016), SM2H.6.
21. J. Henningsen, J. Hald, and J. C. Petersen, "Saturated absorption in acetylene and hydrogen cyanide in hollow-core photonic bandgap fibers," Opt. Express **13**, 10475-10482 (2005).
22. "http://hitran.org/docs/definitions-and-units/", retrieved 8/8/2018.
23. K. Knabe, S. Wu, J. Lim, K. A. Tillman, P. S. Light, F. Couny, N. Wheeler, R. Thapa, A. M. Jones, J. W. Nicholson, B. R. Washburn, F. Benabid, and K. L. Corwin, "10 kHz accuracy of an optical frequency reference based on $^{12}C_2H_2$-filled large-core kagome photonic crystal fibers," Opt. Express **17**, 16017-16026 (2009).
24. R. Thapa, K. Knabe, M. Faheem, A. Naweed, O. L. Weaver, and K. L. Corwin, "Saturated absorption spectroscopy of acetylene gas inside large-core photonic bandgap fiber," Opt. Lett. **31**, 2489-2491 (2006).
25. https://www.openoptogenetics.org/images/5/59/Guide_to_Connectorization_and_Polishing_of_Optical_Fibers.pdf", retrieved 9/25/2018.
26. S. Hosseini-Zavareh, M. P. Thirugnanasambandam, H. W. Kushan Weerasinghe, B. R. Washburn, and K. L. Corwin, "Improved Acetylene-Filled Photonic Bandgap Fiber Cells Fabricated using a Tapering Method," in *Frontiers in Optics / Laser Science*, OSA Technical Digest (Optical Society of America, 2018), JW4A.95.
27. "Telecommunication," https://en.wikipedia.org/wiki/Telecommunication (2018).
28. "Bureau International des Poids et Mesures Recommendation CCL 2c," (2003).
29. Mircea Gheorghiu, "Advanced Chemical Experimentation and Instrumentation," Massachusetts Institute of Technology: MIT http://web.mit.edu/5.33/www/Exp1_IR_05.pdf(2007).
30. P. F. Bernath, "Spectra of atoms and molecules," Oxford university press (1995).
31. J. B. Anderes Bjarklev, Araceli Sanchez Bjarklev, "Photonic crystal fibers," Kluwer academic publishers (2003).
32. F. Benabid, P. J. Roberts, F. Couny, and P. S. Light, *Light and gas confinement in hollow-core photonic crystal fibre based photonic microcells*, 2009 (2009), Vol. 4.
33. M. S. Newville, Till; Allen, Daniel B.; Ingargiola, Antonino, "LMFIT: Non-Linear Least-Square Minimization and Curve-Fitting for Python," https://lmfit.github.io/lmfit-py.
34. "http://www.spectralcalc.com/info/about.php", retrieved 8/8/2018.